

## إقرار

أنا الموقع أدناه مقدم الرسالة التي تحمل العنوان:

المشاركة المثالية والتحكم في الطاقة في الشبكات الذكية

Optimized control and power sharing in microgrid network

أقر بأن ما اشتملت عليه هذه الرسالة إنما هو نتاج جهدي الخاص، باستثناء ما تمت الإشارة إليه حيثما ورد، وإن هذه الرسالة ككل أو أي جزء منها لم يقدم من قبل لنيل درجة أو لقب علمي أو بحثي لدى أي مؤسسة تعليمية أو بحثية أخرى.

### DECLARATION

The work provided in this thesis, unless otherwise referenced, is the researcher's own work, and has not been submitted elsewhere for any other degree or qualification

Student's name: Mohammed Jouda

اسم الطالب: محمد سعيد جودة

Signature: Mohammed Jouda

التوقيع: محمد سعيد جودة

Date: 20/6/2015

التاريخ: 2015/6/20



# OPTIMIZED CONTROL AND POWER SHARING IN MICROGRID NETWORK

**Mohammed S. Jouda**  
**120130423**

A thesis report submitted in partial  
fulfillment of the requirement for the award of the  
Degree of Master of Electrical Engineering

*Supervisor:*

**Dr. Basel Hamed**  
Islamic University of Gaza  
Gaza, Gaza Strip

June 2015



## نتيجة الحكم على أطروحة ماجستير

بناءً على موافقة شئون البحث العلمي والدراسات العليا بالجامعة الإسلامية بغزة على تشكيل لجنة الحكم على أطروحة الباحث/ محمد سعيد سلمان جودة لنيل درجة الماجستير في كلية الهندسة قسم الهندسة الكهربائية - أنظمة التحكم وموضوعها:

### المشاركة المثالية والتحكم في الطاقة في الشبكات الذكية

### Optimized control and power sharing in microgrid network

وبعد المناقشة العلنية التي تمت اليوم السبت 26 شعبان 1436هـ، الموافق 2015/06/13م الساعة الحادية عشرة صباحاً بمبنى القدس، اجتمعت لجنة الحكم على الأطروحة والمكونة من:

د. باسل محمود حمد مشرفاً ورئيساً  
د. حاتم علي العايدي مناقشاً داخلياً  
د. محمد حاتم مشتهى مناقشاً خارجياً

وبعد المداولة أوصت اللجنة بمنح الباحث درجة الماجستير في كلية الهندسة / قسم الهندسة الكهربائية -

### أنظمة التحكم.

واللجنة إذ تمنحه هذه الدرجة فإنها توصيه بتقوى الله ولزوم طاعته وأن يسخر علمه في خدمة دينه ووطنه.

والله والوفيق،،،

مساعد نائب الرئيس للبحث العلمي والدراسات العليا

إ.د. فؤاد علي العاجز



# DEDICATION

*This thesis is dedicated to:*

*The sake of Allah, my Creator and my Master,  
My great teacher and messenger, Mohammed (May Allah bless and  
grant him), who taught us the purpose of life,  
The Islamic University; my second magnificent home;  
My great Supervisor Dr. Basel Hamed, who First of helped me and put  
me on the right path,  
My great parents, who never stop giving of themselves in countless ways,  
My dearest wife, who leads me through the valley of darkness,  
My sweet daughter KINDA, who I can't force myself to stop loving,  
To My beloved brothers and sisters,  
To all my family, the symbol of love and giving,  
with light of hope and support,  
My friends who encourage and support me,  
All the people in my life who touch my heart,  
I dedicate this research..*

# ACKNOWLEDGMENTS

*First and foremost, I must acknowledge my limitless thanks to Allah, the Ever-Magnificent; the Ever-Thankful, for His help and bless. I am totally sure that this work would have never become truth, without His guidance.*

*I owe a deep debt of gratitude to our university for giving us an opportunity to complete this work.*

*I am grateful to my supervisor, Dr. Basel Hamed,, who worked hard with me from the beginning till the completion of the present research particularly who has been always generous during all phases of the research, and I highly appreciate the efforts expended by Dr. Basel.*

*I would like to take this opportunity to say warm thanks to all my beloved friends, who have been so supportive along the way of doing my thesis.*

*I also would like to express my wholehearted thanks to my family for their generous support they provided me throughout my entire life and particularly through the process of pursuing the master degree. Because of their unconditional love and prayers, I have the chance to complete this thesis.*

# ABSTRACT

An important issue of microgrid is to share the load demand, the structure of the research. Two parallel inverters with load system are presented. The paralleled inverters need to work in grid-connected mode and stand-alone mode, and to switch seamlessly between the two modes. For a networked microgrid configuration with linear and nonlinear loads, the reactive power sharing is more challenging. For improvement of reactive power sharing and control in networked microgrid, a control method is introduced to reduce reactive power sharing errors by Droop control method is a widely used technique for achieving load sharing in microgrid applications. To achieve load sharing between parallel inverters, this control strategy combines frequency and voltage droop method and inverter voltage regulation control scheme.

The droop methods are introduced to share real and reactive power in microgrid. The improvement of the droop control is made to obtain a more stable voltage and better load sharing between two parallel inverters. The performance of the control strategy is verified in simulation using Matlab/Simulink.

To solve the power sharing control issues, the particle swarm optimization with the frequency-voltage droop control methods have been proposed. The real and reactive power are developed. In order to improve the stability of the microgrid system.

# LIST OF CONTENTS

<b>CHAPTER1 INTRODUCTION</b> .....	1
1.1 Introduction: .....	1
1.2 The research problem:.....	2
1.3 Related Work: .....	2
1.4 The objectives of the study:.....	5
1.5 Scope of the study: .....	5
1.6 Contribution:.....	6
1.7 Outline of the thesis: .....	6
<b>CHAPTER2 INTRODUCTION OF POWER ELECTRONICS</b> .....	7
2.1 Introduction: .....	7
2.2 Basics of Power processing:.....	7
2.2.1 AC-DC conversion: .....	7
2.2.1.1 Uncontrolled Rectifiers:.....	8
2.2.1.2 Phase-controlled Rectifiers.....	10
2.2.2 DC-DC conversion: .....	11
2.2.3 DC-AC conversion: .....	13
2.2.3.1 Single Phase Inverter: .....	14
2.2.3.2 Three-phase Inverters:.....	16
<b>CHAPTER3 MICROGRIDS AND CONTROL SYSTEMS</b> .....	18
3.1 Introduction of control systems: .....	18
3.1.1 PID Control:.....	18
3.1.1.1 Tuning PID controller: .....	22
3.1.1.2 Ziegler-Nichols Tuning: .....	22
3.2 Microgrid Literature:.....	24
3.2.1 Voltage and Current Regulation: .....	24
3.2.2 Power and Energy management: .....	24
3.2.3 Power Sharing:.....	25
3.2.3.1 Master/slave control techniques:.....	26
3.2.3.2 Current/power sharing control techniques:.....	26

3.2.3.3 Frequency and voltage droop control techniques.....	26
3.3 Particle Swarm Optimization: .....	27
<b>CHAPTER4 THE CONTROL INVERTERS FOR PARALLEL OPERATION .....</b>	<b>30</b>
4.1 Introduction: .....	30
4.2 Droop Control: .....	30
4.2.1 Power calculation and equations: .....	31
4.2.2 Droop control strategy: .....	34
4.2.2.1 Voltage control block:.....	36
4.2.2.2 Current control block :.....	36
4.3 SIMULATION RESULTS: .....	37
4.3.1 case I: .....	42
4.3.2 case II: .....	43
4.3.3 Results of PSO: .....	45
<b>CHAPTER5 CONCLUSION AND FUTURE WORK .....</b>	<b>47</b>
5.1 Conclusion:.....	47
5.2 Future Work:.....	47
<b>REFERENCES: .....</b>	<b>48</b>
<b>APPENDIX A.....</b>	<b>50</b>
<b>APPENDIX B.....</b>	<b>52</b>
<b>APPENDIX C .....</b>	<b>54</b>



## LIST OF TABLES

<i>Table 3.1 Summarize The PID Techniques .....</i>	<i>22</i>
<i>Table 3.2 Tuning of PID Controller Parameter According to Z-N Tuning.....</i>	<i>23</i>
<i>Table 3.3 Tuning of PID Controller Parameter According to Second Z-N Tuning .....</i>	<i>23</i>
<i>Table 4.1 Filtre Parameter Values of The Inverter .....</i>	<i>37</i>
<i>Table 4.2 Simulation Parameters .....</i>	<i>39</i>

## LIST OF FIGURES

<b>Figure 1.1</b> General Structure of Microgrid .....	1
<b>Figure. 1.2</b> Inverter Control Scheme [6]. .....	4
<b>Figure 1.3</b> Inverter Control Scheme.....	4
<b>Figure 1.4</b> Microgrid Scheme .....	5
<b>Figure 2.1</b> Sketch of Power Processing .....	7
<b>Figure 2.3</b> Uncontrolled Rectifier With Bridge .....	9
<b>Figure 2.4</b> Uncontrolled Three-Phase Bridge Rectifier .....	9
<b>Figure 2.5</b> Phase-Controlled Rectifier With Inductive Load .....	10
<b>Figure 2.6</b> Buck Converter.....	11
<b>Figure 2.7</b> Boost Converter .....	12
<b>Figure 2.8</b> General Block Diagram .....	13
<b>Figure 2.9</b> Half Bridge Inverter Diagram.....	14
<b>Figure 2.10</b> Full Bridge Inverter (H-Bridge inverter) .....	15
<b>Figure 2.11</b> Sinusoidal PWM (SPWM) .....	15
<b>Figure 2.12</b> Operation Of Single Phase Inverter .....	16
<b>Figure 2.13</b> Three Phase Inverter .....	16
<b>Figure 2.14</b> Voltage Waveforms Output by a 3-Phase Square Wave .....	17
<b>Figure 3.1</b> Block Diagram of PID Controller .....	18
<b>Figure 3.2(a)</b> Step Response of Kp Controller .....	20
<b>Figure 3.2(b)</b> Root Locus of Kp Controller .....	20
<b>Figure 3.3</b> Step Response of PI Controller .....	21
<b>Figure 3.4</b> Step Response of PID Controller.....	21
<b>Figure 3.5</b> Response Curve for Ziegler-Nichols (First Method).....	22
<b>Figure 3.6</b> Step Response for System Tuned Via the Second Method .....	24
<b>Figure 3.7</b> Hierarchical Operation Modes of the Flexible Microgrid .....	25
<b>Figure 3.8</b> Simplified Grid Connected Microgrid With Multiple Distributed Generators.....	25
<b>Figure 3.9</b> Master/Slave Configuration.....	26
<b>Figure 3.10</b> Reference Voltage and Power Calculation.....	27
<b>Figure 3.11</b> Inverter Control Scheme with Droop Control .....	27
<b>Figure 3.12</b> Concept of Modification of Searching Point by PSO.....	28
<b>Figure 3.13</b> Searching Concepts with Agents in Solution Space by PSO. ....	29

<b>Figure 3.14</b> Particle Swarm Optimization Flow Chart .....	29
<b>Figure 4.1</b> Two Inverters Connected in Parallel .....	30
<b>Figure 4.2</b> Equivalent Model of Voltage Source Inverter.....	31
<b>Figure 4.3(a)</b> Frequency Droop Control .....	33
<b>Figure 4.3(b)</b> Voltage Droop Control .....	34
<b>Figure 4.4</b> Full Bridge Inverter System. ....	34
<b>Figure 4.5</b> Parallel Structure of Two Inverter Modules.....	35
<b>Figure 4.6</b> Two Inverters in Microgrid. ....	35
<b>Figure 4.7</b> Voltage PI Compensator.....	36
<b>Figure 4.8</b> Current PI Compensator .....	36
<b>Figure 4.9.</b> Voltage- and Current-Loop Control Structure.....	36
<b>Figure 4.10</b> Reference Voltage and Power Calculation.....	37
<b>Figure 4.11</b> Control strategy of parallel inverter modules .....	38
<b>Figure 4.12</b> Design sinusoidal inverter .....	39
<b>Figure 4.13</b> Operation of Single Phase Inverter.....	40
<b>Figure 4.12</b> Output Phase Voltage .....	40
<b>Figure 4.14</b> Distributed Generation (Inverter design) by Matlab .....	41
<b>Figure 4.15</b> Active Power of Inverters 1 and 2 .....	42
<b>Figure 4.16</b> Frequency of Inverters 1 and 2 .....	42
<b>Figure 4.17</b> Power Sharing Performance. ....	43
<b>Figure 4.18</b> Power Sharing Performance .....	44
<b>Figure 4.19</b> Design Particle Swarm Optimization .....	45
<b>Figure 4.20</b> Power Sharing Performance with PSO.....	46

### 1.1 Introduction:

The concept of the microgrid has emerged in response to the increased penetration of renewable energy systems. Thus make progress and complacency our future energy demands will easily be met, by new technology that will be supported for distributed generation (DG) units by microgrids. The microgrids are applied on different types of loads and some of sources.

The total power sharing of the load demand by distributed generation units or inverters must equal share load to make stability of power sharing and control it. In this research, we will use the voltage and frequency droop control method for sharing active and reactive power from multiple distributed generation units. These (DG) units can be expressed by some devices as (inverters and storage units “battery”...), where the parallel inverters in microgrids need to work in grid connection and island (stand-alone) mode.

According to the microgrid concepts, the general structure as shown in Figure 1.1, Distributed generation (DG), storage units or energy storage system (ESS), and the loads are assembled as parallel devices connected in the main grid by static transfer switch (STS).

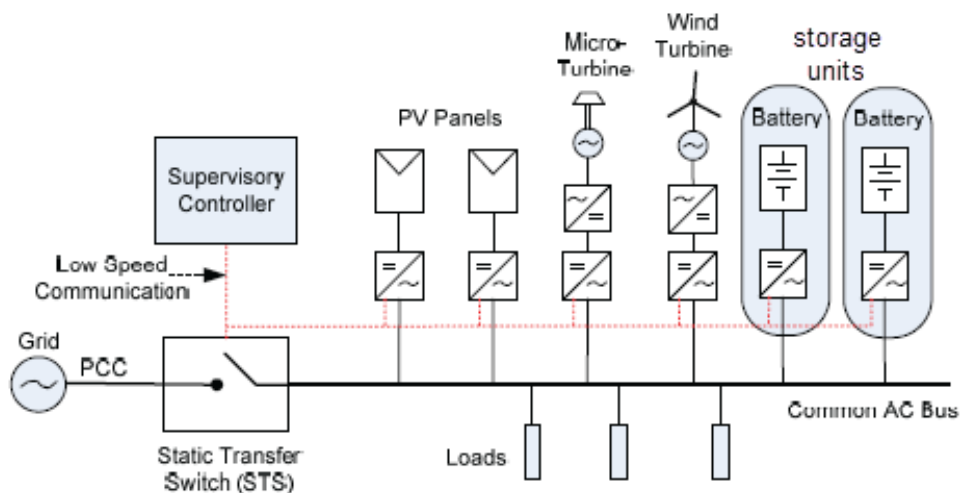


**Figure 1.1** General Structure of Microgrid

The STS is used to isolate the microgrid from the main grid at the point of common coupling (PCC). ESS can be used to balance any error or mismatch between the power sources and loads demand. It is necessary to avoid any interruption from power sources, and to be able to convert from grid connection mode to stand-alone mode (island mode) and vice versa.

In distributed generation (DG) systems, the uninterruptable power supply (UPS) of the systems, may be more than one inverter applied in parallel. Therefore, the parallel operation of inverters with other inverters, and with the main grid, are very sensitive to disturbances

from the load or other sources and can easily be damaged by over current. Hence, careful attention should be given to system design and the control of parallel operation of inverters. When two or more inverters operate in parallel, the following features must be achieved: [1]

- (1) Amplitude, frequency and phase synchronization among the output voltages of inverters,
- (2) The priority current distribution according to the capacities,
- (3) Flexibility and
- (4) Very high switching feature at any time

## 1.2 The research problem:

Inverters may have to be operated in parallel directly or indirectly. How to share the load among the inverters operated in parallel is a challenging problem. The sharing power for the loads demand by using multiple distributed generation (DG) systems, the total sharing by paralleled inverters must be equal share to the demand load to make stability of power systems. However, only used for linear load, but for nonlinear load, the harmonics component and the transient power, it's prevent sharing rightly. [2]

A voltage and frequency droop control methods for parallel inverter connected are used for sharing real and reactive power from multiple distributed generation (DG) units. The real power sharing in microgrids is always accurate, but the reactive power sharing is very sensitive. The reactive power sharing accuracy in a simplified microgrid with two distributed generation (DG) units has been introduced in many literatures. [3] [4]

The types of connection between the parallel inverters:

1. Wire communication (Master-Slave or current chain scheme).
2. Droop Control.

The first type, if one of the parallel inverters disconnect to the others. In this case will affect the network. But the droop control method for the parallel inverters can avoid the communication between them. With no connection between the inverters, the output of voltage for each inverter is not stable and no sharing to the load. The inverters need to control the voltage and sharing loads. A natural problem for parallel-operated inverters is how to share the load among.

## 1.3 Related Work:

In (Tuladhar et al. 1997) and a small signal injection method was proposed to improve the reactive power sharing accuracy in (Tuladhar et al. 2000), which can also be extended to harmonic current sharing. Injecting a harmonic voltage according to the output harmonic current can be used to improve the total harmonic distortion (THD) of the voltage (Borup et al. 2001).

In (Guerrero et al. 2004, 2005), it was pointed out that the output impedance of inverters could play an important role in power sharing and a droop controller for inverters with resistive output impedances was proposed for sharing linear and non-linear loads (Guerrero et al. 2006a, 2007).

In "C.-C. Hua, K.-A.L., J.-R. Lin, Parallel operation of inverters for distributed photovoltaic power supply system" [5], the paper proposes a control technique for operating two or more

single-phase inverter modules in parallel with no auxiliary interconnections. In the proposed parallel inverter system, each module includes an inner current loop and an outer voltage loop controls, this technique is similar to the conventional frequency/voltage droop concept using frequency and fundamental voltage droop to allow all independent inverters to share the load in proportion to their capacities. However, the paper considered only inductive lines.

Although significant progress has been made for the equal sharing of linear and nonlinear loads, it was reported that the accuracy of reactive power sharing (for the  $Q - E$  and  $P - \omega$  droop) is not high (Guerrero et al. 2006b; Lee et al. 2010; Li and Kao 2009). Moreover, some approaches developed for equal sharing, e.g. the one proposed in (Marwali et al. 2004), cannot be directly applied to proportional sharing. Another issue is that the output voltage drops due to the increase of the load and also due to the droop control (Sao and Lehn 2005).

Adding an integral action to the droop controller is able to improve the accuracy of load sharing for grid-connected inverters (Dai et al. 2008a; Li et al. 2004; Marwali et al. 2004) but it does not work for inverters operated in the stand-alone mode and also there is an issue associated with the change of the operation mode. Adding a virtual inductor and estimating the effect of the line impedance is able to improve the situation by changing the droop coefficients (Li and Kao 2009). A  $Q-V$  dot droop control method was proposed in (Lee et al. 2010) to improve the accuracy of reactive power sharing following the idea of changing the droop coefficients in (Li and Kao 2009) but a mechanism to avoid the output voltage variation was necessary, which reduces the accuracy of the reactive power sharing, as can be seen from the results given there. These strategies are sensitive to numerical computational errors, parameter drifts and component mismatches.

Other trends to solve the power sharing problems for parallel-operated inverters are to make the output impedance as accurate as possible over a wide range of frequencies (see (Guerrero et al. 2008; Yao et al. 2011) and the references therein) and to introduce the secondary control to bring the deviated voltage and frequency back to the rated values (Guerrero et al. 2009, 2011). However, this inevitably needs communication among the inverters (even of low bandwidth) and the advantage of droop control is lessened. The secondary control also leads to slow responses and/or instability because of the delay introduced in the measurement and communication channel. The complexity of the system is also increased, as evidenced by the number of control loops/levels involved in such systems. This, again, increases the chance of instability.

In “M.C. Chandorkar, D.M. Divan, R. Adapa” [6], Control of parallel connected inverters in standalone AC supply systems, scheme for controlling parallel connected inverters in a stand-alone ac supply system is presented, see Figure. 1.2, this scheme is suitable for control of inverters in distributed source environments such as in isolated AC systems, large UPS systems, and PV systems connected to AC grids. Active and reactive power sharing between inverters can be achieved by controlling the power angle (by means of frequency), and the fundamental inverter voltage magnitude. The control is done in the d-q reference frame; an inverter flux vector is formed by integrating the voltage space vector. The choice of the switching vectors is essentially accomplished by hysteresis comparators for the set values and then using a look-up table to choose the correct inverter output voltage vector. The considerations for developing the look-up table are dealt with in “I. Takahashi, T. Noguchi, A new quick-response and high-efficiency control strategy of an induction motor” [7]. However, the inductance connected between the inverter and the load makes the output impedance high. Therefore, the voltage regulation as well as the voltage waveform quality is

not good under load change conditions as well as nonlinear load condition. The authors explain the same concept but with focusing in control issues of UPS systems in [8].

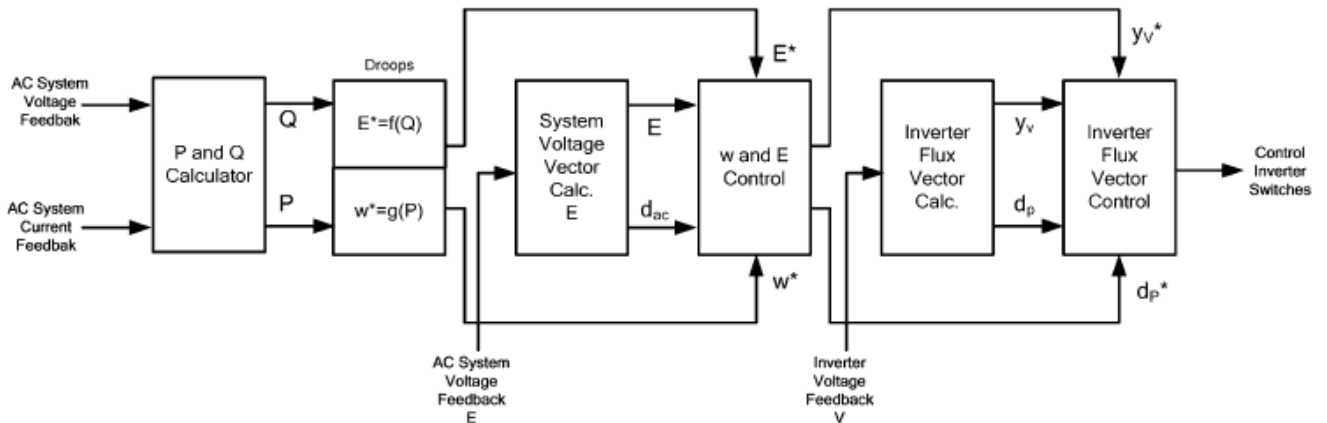


Figure. 1.2. Inverter Control Scheme [6].

In “ the S.H. Hauck Matthias and Wechselrichter problemlos” [9,10] , the inverse droop equations are used to control the inverter. The inverter is able to work in parallel with a constant voltage constant-frequency system, as well as with other inverters or also in stand-alone mode. There is no communication interface needed. The different power sources can share the load also under unbalanced conditions. Very good load sharing is achieved by using an outer control loop with active and reactive power controller, for which the set point variables are derived out of droops. Furthermore, a relatively big inductance of 12mH (C=10uF) is used in the LC filter and a small decoupling reactance is used to decouple the inverter from other voltage sources. The interface inductance The authors address here UPS applications and renewable energy systems. See Figure. 1.3.

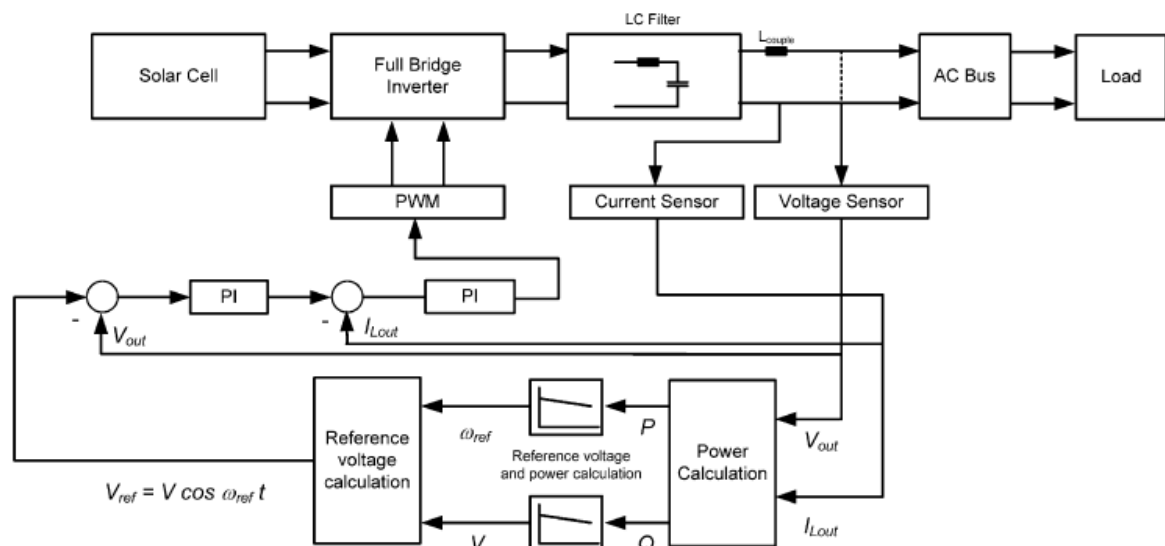


Figure. 1.3. Inverter Control Scheme [9].

## 1.4 The objectives of the study:

To improve the microgrid power sharing with linear loads and nonlinear loads, and the main objective of the research is to design the control of parallel inverters in stand-alone mod, and applied the P-W and Q-V droop control where the inverter frequency and voltage amplitude are drooped linearly with the inverter output active and reactive power, respectively. Improvement of droop control will keep the stability in voltage and frequency to have a better of power sharing.

## 1.5 Scope of the study:

1. Design the pure sine wave inverters.
2. Design the parallel inverter with load.
3. Design the droop control method to control the parallel inverter.
4. To get better voltage and power sharing between parallel inverters.
5. Design droop control with particle swarm method.

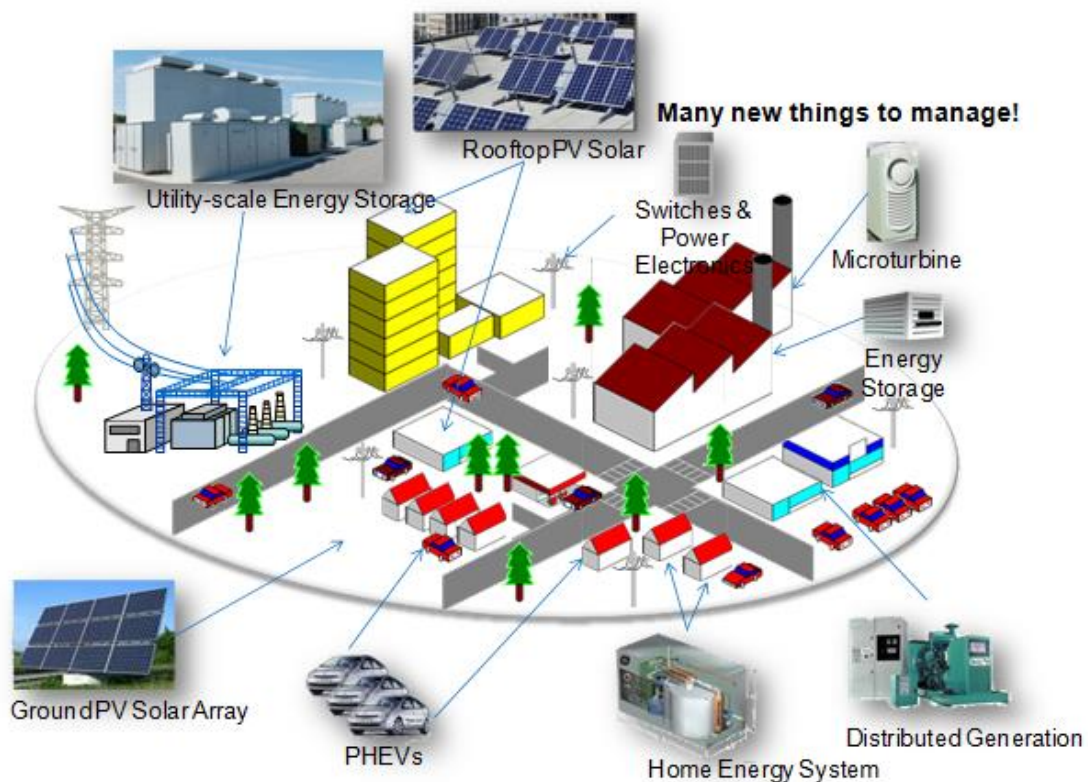


**Figure 1.4** Microgrid Scheme

As shown in a Figure 1.4, a simple definition of a microgrid is an independent energy system providing grid backup or off-grid power, These (DG) units can be expressed by some devices as (inverters and storage units “battery”...), where the parallel DG in microgrids need to work in grid connection and island (stand-alone) mode.



## 1.6 Contribution:

The main task of this research is to design the control of the parallel inverter system of standalone microgrid, and the droop control is applied to achieve good load sharing with low voltage and frequency deviation in microgrid. Improvement of the droop control is to keep the voltage more stable meanwhile to get a better reactive power sharing.

Design a microgrid that has the potential to:

- Increase the amount of renewable energy contributing to power needs, both locally and on the overall grid,
- Combine renewable and other power sources,
- Provide power in places where there is no grid,
- Provide more reliable power in places served by a grid,
- Increase the stability and reliability of the power grid.

## 1.7 Outline of the thesis:

After making an introduction in this chapter, the thesis is divided into five chapters: we will present in chapter 2, an overview and some basics about power processing and some hardware issues relevant to the design of power inverters. Chapter 3 is devoted to literature of microgrids and control system with PID control. In Chapter 4, the parallel operation of inverters is discussed. And presenting the conventional droop control strategies for inverters, the limitations of the conventional droop control are revealed. The accuracy of power sharing greatly depends on the accuracy and consistency of the components, and the voltage regulation capability is poor. Then, particle swarm optimization control strategies for inverters are presented so that accurate sharing of both real power and reactive power can be achieved even if there are component mismatches, numerical errors, disturbances and noises, etc. the conclusion and future works are presented in Chapter 5.

### 2.1 Introduction:

In this chapter, a general review followed by some basics of power electronics and some hardware issues to the design of power inverters. Relevant to smart grid integration and solar power systems, power electronics is the technology associated with efficient conversion and control of electric power by using power semiconductor devices. On other hand, according to IEEE Power Electronics Society, the application of circuit theory, design techniques, and the development of analytical tools toward efficient electronic conversion, control, and conditioning of electric power.

### 2.2 Basics of Power processing:

Power electronics contain four types of power processing: AC-DC conversion, DC-DC conversion, DC-AC conversion and AC-AC conversion, we can use power electronics to convert a source into another supply to be suitable for the load, as shown in Figure 2.1. There are many books on subject of power electronics. [11]

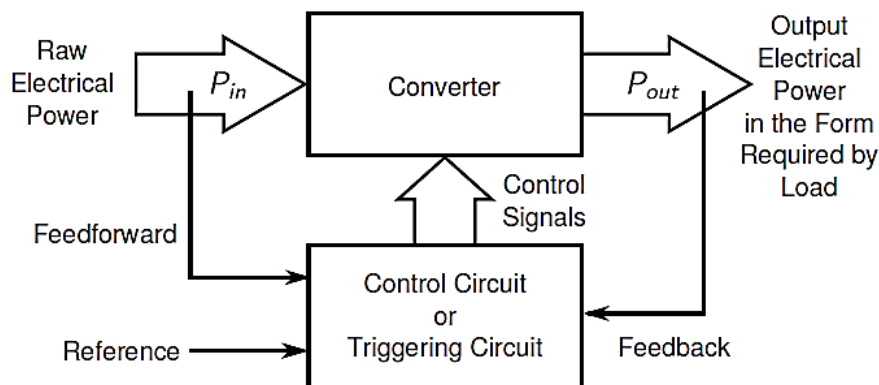


Figure 2.1 Sketch of Power Processing

#### 2.2.1 AC-DC conversion:

AC to DC is often called rectification, so we will expect the output voltage is a pure DC signal without any ripples and the input current is in phase with the voltage and does not have harmonics, rectifiers can be divided into:

- (1) Uncontrolled rectifiers with diodes,
- (2) Phase-controlled rectifiers with thyristors and PWM-controlled rectifiers with IGBTs or MOSFETs.

### 2.2.1.1 Uncontrolled Rectifiers:

The simplest rectifier, which consists of a diode, as shown in Figure 2.2

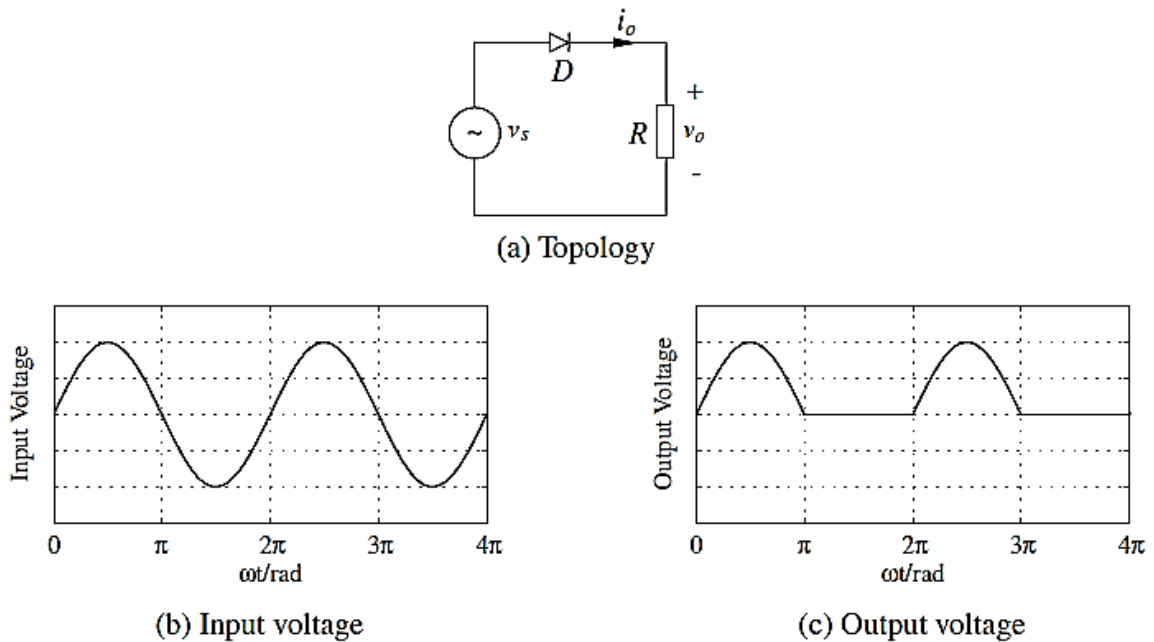
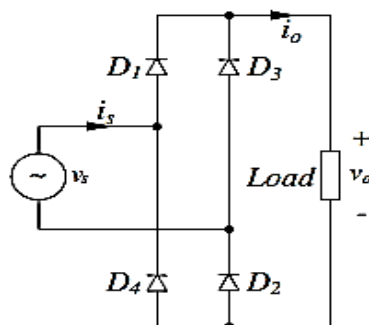


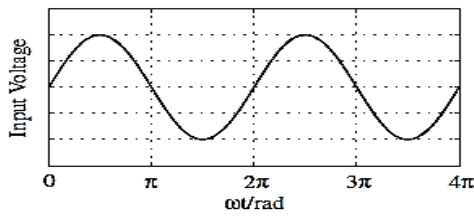
**Figure 2.2** Uncontrolled Rectifier With Diode

Half cycle of the input voltage can pass the diode to reach the load and, hence, the output voltage is of DC but with a significant amount of ripples. To reduce the ripples in the output voltage and to reduce the harmonics in the input current, several diodes are often connected to form bridge rectifiers. Figure 2.3 shows a single-phase bridge rectifier and its operation principle. Compared to the rectifier with one diode shown in Figure 2.2(a), both half cycles of the input voltage are passed to the load. As a result, the ripples in the output voltage are reduced and the harmonic components in the input current are reduced as well. In this case, the DC output voltage is

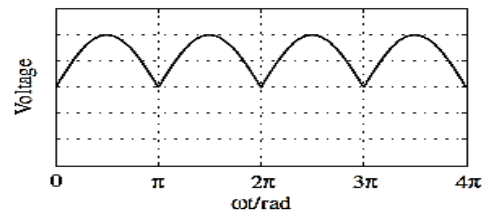
$$V_o = \frac{1}{\pi} \int_0^{\pi} \sqrt{2} V_s \sin \omega t d(\omega t) = \frac{2\sqrt{2}}{\pi} V_s \approx 0.9V_s \dots\dots\dots(2.1)$$



(a) Topology



(b) Input Voltage

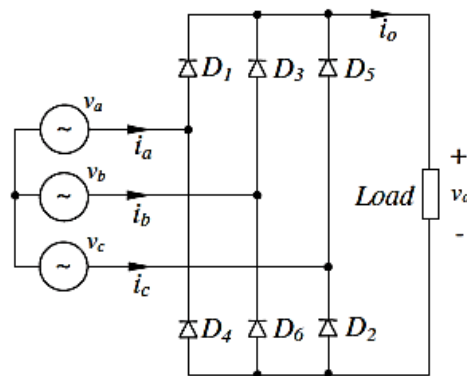


(c) Output Voltage

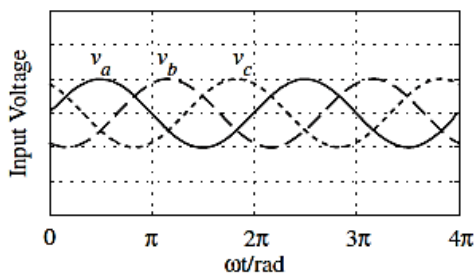
Figure 2.3 Uncontrolled Rectifier With Bridge

For three-phase applications, the bridge rectifier shown in Figure 2.4 can be adopted. The pair of diodes with the highest instantaneous line voltage conduct, in the order of D1D2 → D2D3 → D3D4 → D4D5 → D5D6 → D6D1 → D1D2 for 120° each time. Hence, the output voltage is the envelope of the line voltages with six ripples, which further improves the performance of the DC output voltage. In this case, the DC output voltage is

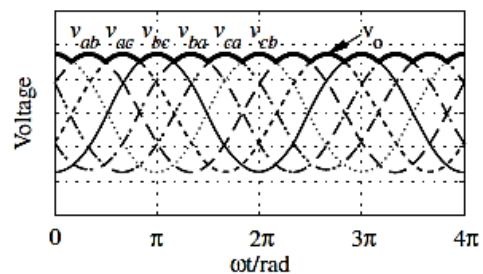
$$V_0 = \frac{1}{\pi/6} \int_0^{\pi/6} \sqrt{2} \times \sqrt{3} V_S \cos \omega t d(\omega t) = \frac{3\sqrt{6}}{\pi} V_S \approx 2.34 V_S \dots \dots \dots (2.2)$$



(a) Topology



(b) Input voltages



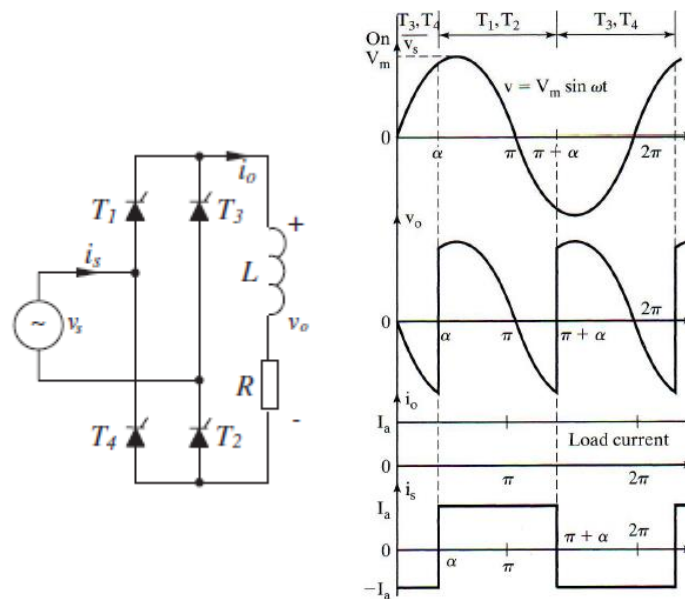
(c) Output voltage

Figure 2.4 Uncontrolled Three-Phase Bridge Rectifier

### 2.2.1.2 Phase-controlled Rectifiers

The thyristor phase-controlled rectifier is widely used for obtaining variable dc voltage from a constant ac voltage and frequency source, but the Diode rectifiers can only provide fixed output voltages. The output voltage of a phase-controlled rectifier can be changed by varying the firing angle of the thyristors.

The variable dc voltage from the phase-controlled rectifiers, (often with an efficiency above 95%), are widely used in many industrial applications, especially in variable-speed drives of DC motors. Figure 2.5 shows a phase-controlled full-bridge rectifier and its operation. During the positive half-cycle of the input voltage, thyristors T1 and T2 are forward biased and negative. Similarly, during the negative half-cycle of the input voltage, thyristors T3 and T4 are forward biased and the voltage is rectified. [12]



**Figure 2.5** Phase-Controlled Rectifier With Inductive Load

It can be seen that from the firing angle  $\alpha$  to  $\pi$ , the input voltage  $V_s$  and input current  $i_s$  are positive so the energy flows from the source to the load. However, during the period from ( $\pi$  to  $\pi + \alpha$ ), the input voltage  $V_s$  is negative and the input current is positive. Hence, the energy (stored in the large inductor) flows backwards.

The DC output voltage is

$$V_0 = \frac{1}{\pi} \int_{\alpha}^{\alpha+\pi} \sqrt{2} V_s \sin \omega t d(\omega t) = \frac{2\sqrt{2}}{\pi} V_s \cos \alpha \dots \dots \dots (2.3)$$

Thus, the output dc voltage is function of the delay angle  $\alpha$

$$V_0 = \frac{2\sqrt{2}}{\pi} V_s \text{ to } 0 \text{ for } \alpha = 0 \text{ to } \frac{\pi}{2} \dots \dots \dots (2.4)$$

The circuit can be operated in the inversion mode to feed energy to the grid if a negative voltage supply is present on the DC bus. In this case,  $\alpha$  can be changed between

$$\alpha = \frac{\pi}{2} \text{ to } \pi$$

### 2.2.2 DC-DC conversion:

A DC chopper circuit is used to convert fixed dc voltage to a variable dc voltage ( to change the level of voltage from one to another ) . A dc chopper is used to control the speed of a dc motor from power dc supply. The converter can be designed to (reduce or increase) the level of voltage or both. The conversion ratio ( $N$ ) between the output and the input voltage is decide the type of dc conversion. [13]

$N$  is lower than 1, the converter is called a **buck converter**;

When  $N$  is higher than 1, the converter is called a **boost converter**;

When  $N$  can be higher or lower than 1, the converter is called a **buck-boost converter**.

#### ➤ *Buck Conversion:*

Buck converter is a step-down converter, which is shown in Figure 2.6a, the equivalent circuits during switch-on and –off periods are shown in Figures 2.6b and c. Its output voltage and output current.

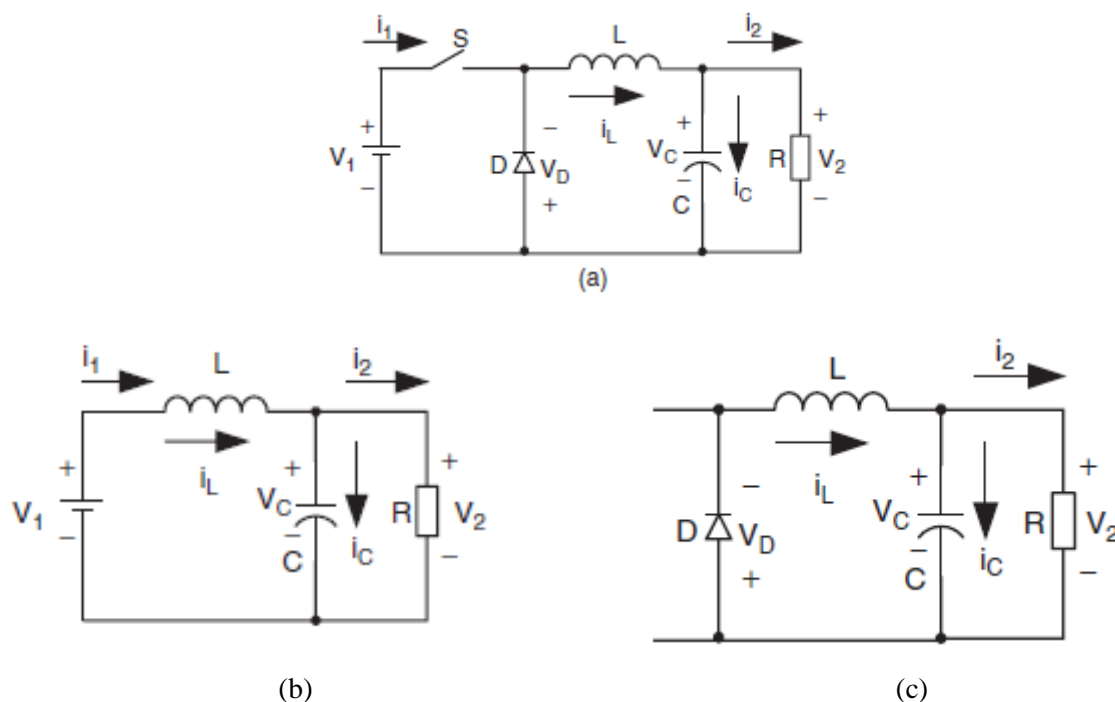


**Figure 2.6** Buck Converter: (a) Circuit Diagram; (b) Switch-on Equivalent Circuit; and (c) Switch-off Equivalent Circuit

We use the inductor and the capacitors in this circuit as a filter to improve the output voltage and current. The switch “S” is turned ON and OFF, and the switching period (T) and the duty cycle is (D), and the ON time is (D\*T), the OFF time in one period (1- D)\*T. The circuit has two operation modes: Mode 1 when the switch “S” is turned ON and Mode 2 when the switch “S” is turned OFF. Both modes are shown in Figures 2.6(b) and 2.6(c), respectively.

$$L \frac{di}{dt} = V1 - V2 \dots\dots\dots (2.5)$$

$$\Delta tc = \frac{V1-V2}{L} \cdot (D\%). (T) \dots\dots\dots (2.6)$$

$$\Delta to = \frac{0-V2}{L} \cdot (1 - D\%). (T) \dots\dots\dots (2.7)$$

**Where**

*Δtc is the rate of change current at closed switch , and Δto is the rate of change current at open switch.*

At steady state:  $\Delta tc + \Delta to = 0$

$$\frac{V1-V2}{L} \cdot (D\%). (T) = \frac{0-V2}{L} \cdot (1 - D\%). (T) \dots\dots\dots (2.8)$$

From equation (2.8), the output voltage is:

$$V2 = D * V1 \dots\dots\dots (2.9)$$

Where V2 is output voltage, V1 is Input voltage.

➤ **Boost conversion:**

Boost converter is a step-up converter, which is shown in Figure 2.7a, where the conversion ratio (N) between the output and the input voltage is higher than 1

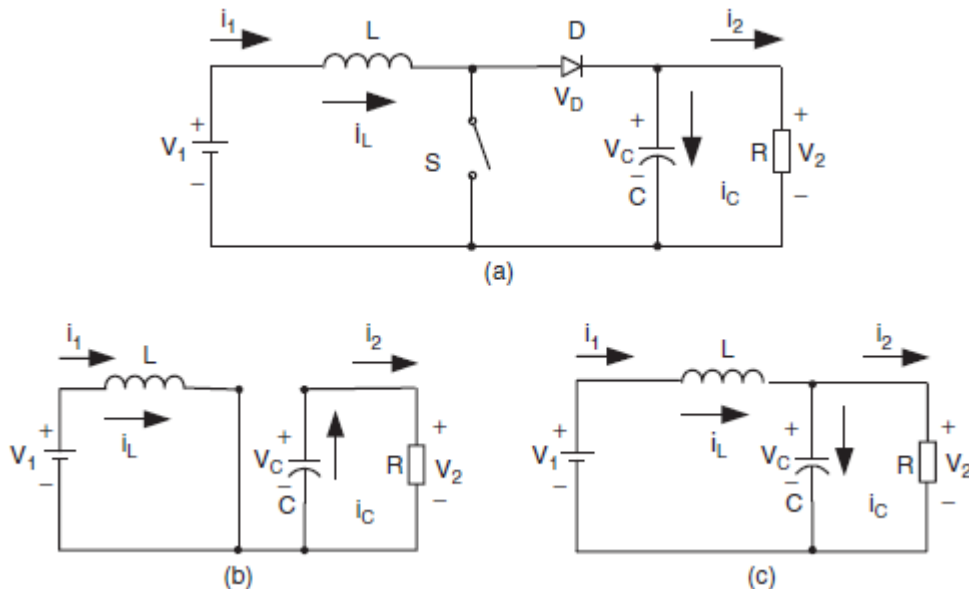


**Figure 2.7** Boost Converter: (a) Circuit Diagram; (b) Switch-on Equivalent Circuit; and (c) Switch-off Equivalent Circuit

There are two operation modes, mode 1 the switch “S” is turned ON and mode 2 the switch “S” is OFF, the equivalent circuits during switch ON and OFF periods are shown in Figures. 2.7b and c.

In mode 1:

$$L \frac{di}{dt} = V_1 \dots\dots\dots (2.10)$$

$$\Delta t_c = \frac{V_1}{L} \cdot (D\%) \cdot (T) \dots\dots\dots (2.11)$$

Where:  $(D\%) \cdot (T) = t_{on}$

At steady state, the energy stores in the inductor will discharge, and the net energy in inductor should be zero in one period.

**In mode 2:**

$$\frac{di}{dt} = \frac{V_1 - V_2}{L} \dots\dots\dots (2.12)$$

$$\Delta t_o = \frac{V_1 - V_2}{L} \cdot (1 - D\%) \cdot (T) \dots\dots\dots (2.13)$$

From equation 2.11 and 2.13:

$$V_2 = \frac{V_1}{1 - D} \dots\dots\dots (2.14)$$

**2.2.3 DC-AC conversion:**

DC-AC converter is called inverter, the power converters to produce an AC output waveform from a DC power supply. DC/AC power converters are widely used today In uninterruptible power supply systems (UPS), AC motor drives, induction heating and renewable energy source systems, speed control of three phase induction and synchronous motors. In Figure 2.8 shows the general block diagram.

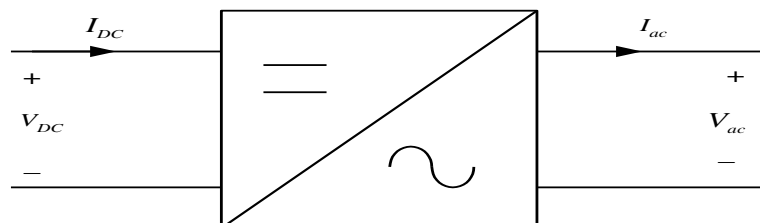


**Figure 2.8** General Block Diagram



The dc to ac inverter are used to convert the following types of input voltages: [14]

1. DC battery voltage to fixed or variable frequency AC voltage (single phase or three phase).
2. AC input voltage rectified to DC, then inverted to single or three phase fixed or variable.

There are a different types of inverters, this depend on the DC supply, the commonly used in the types of inverter is voltage source inverter (VSI) where AC power provides on the output side function as a voltage source. An inverter is a VSI if there is a large capacitor across the DC bus and is a CSI if there is a large inductor in series with the DC supply, is a CSI if there is a large inductor in series with the DC supply. VSI structure are the most widely used because they naturally behave as voltage source as required by many industrial application, such as adjustable speed drives (ASDs), According to the type of the inverter output, an inverter is called current-controlled if the output is controlled to be a current source and voltage-controlled if the output is controlled to be a voltage source. The inverters dealt in this research are VSIs, and we can use a thyristor, IGBT and MOSFET.

### 2.2.3.1 Single Phase Inverter:

#### ➤ *Half Bridge inverter:*

Is the simplest type of single phase inverters, the circuit consist of two transistor Q1, Q2 (e.g. IGBT) connected in series and cross the dc supply. The transistors (Q1, Q2) are turn on and turn off alternately by  $\pi$  to make the output voltage wave, as shown in Figure 2.9

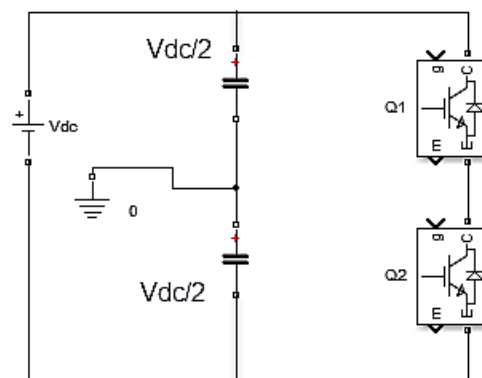
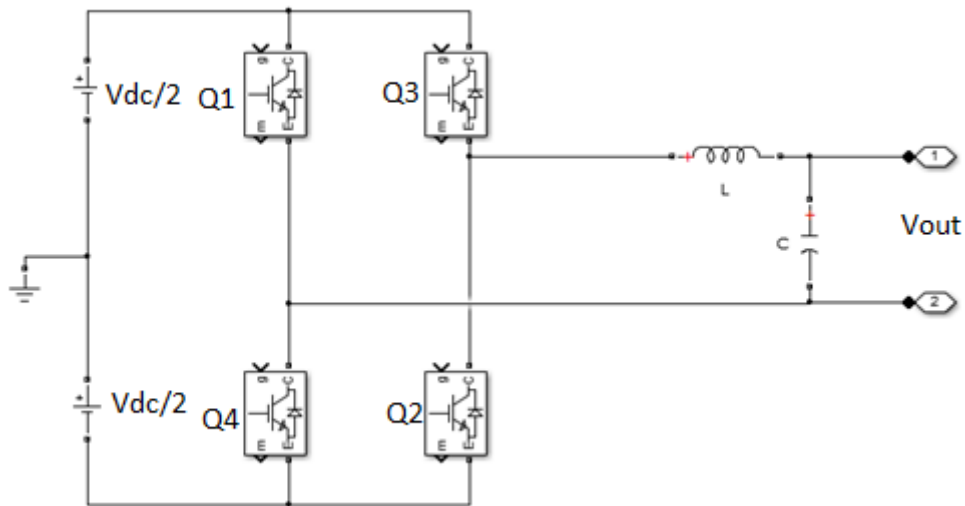


Figure 2.9 Half Bridge Inverter Diagram

#### ➤ *Full Bridge inverter:*

The circuit is consist of two legs or called H-Bridge (two half-bridge), as shown in Figure 2.10, and the load is connected between a and b points, the IGBT's device pairs Q1,Q2 and Q3,Q4 are turned ON and OFF alternately to generate the output voltage and the load current.



**Figure 2.10** Full Bridge Inverter (H-Bridge inverter)

We need to provide a sinusoidal voltage and it is called modulating signal. When the carrier frequency, (switching frequency), is high enough, then the harmonic components can be easily filtered out via a low-pass filter, which is often an LC or LCL filter. This type of modulation is called a sinusoidal PWM (SPWM).

The SPWM is operated on both legs of the inverter as shown in the Figure 2.11, and the same PWM signal is sent to Q1 and Q2 (two phase legs) in complementary way. The result waves are shown in the Figure 2.12 after and before applied the filter, also, Q3 and Q4 is operated PWM at the same time.

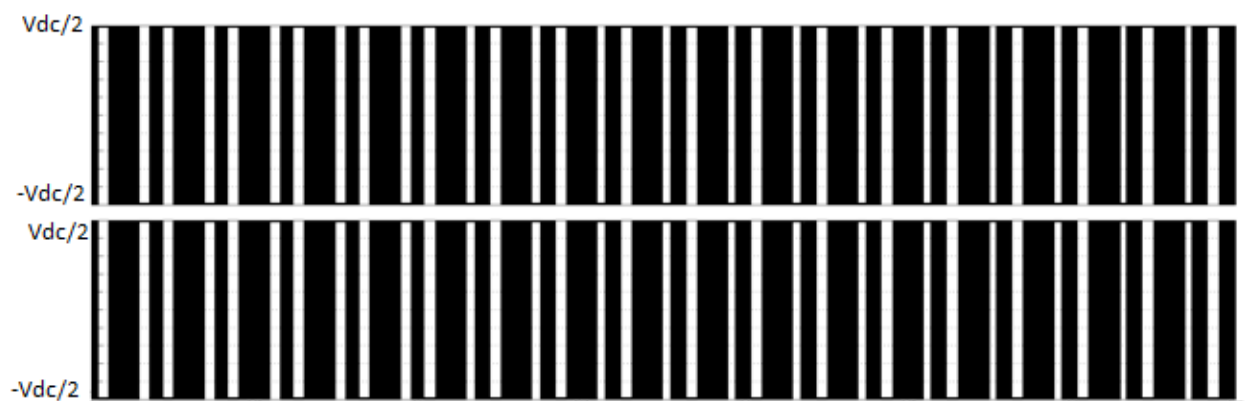


**Figure 2.11** Sinusoidal PWM (SPWM)

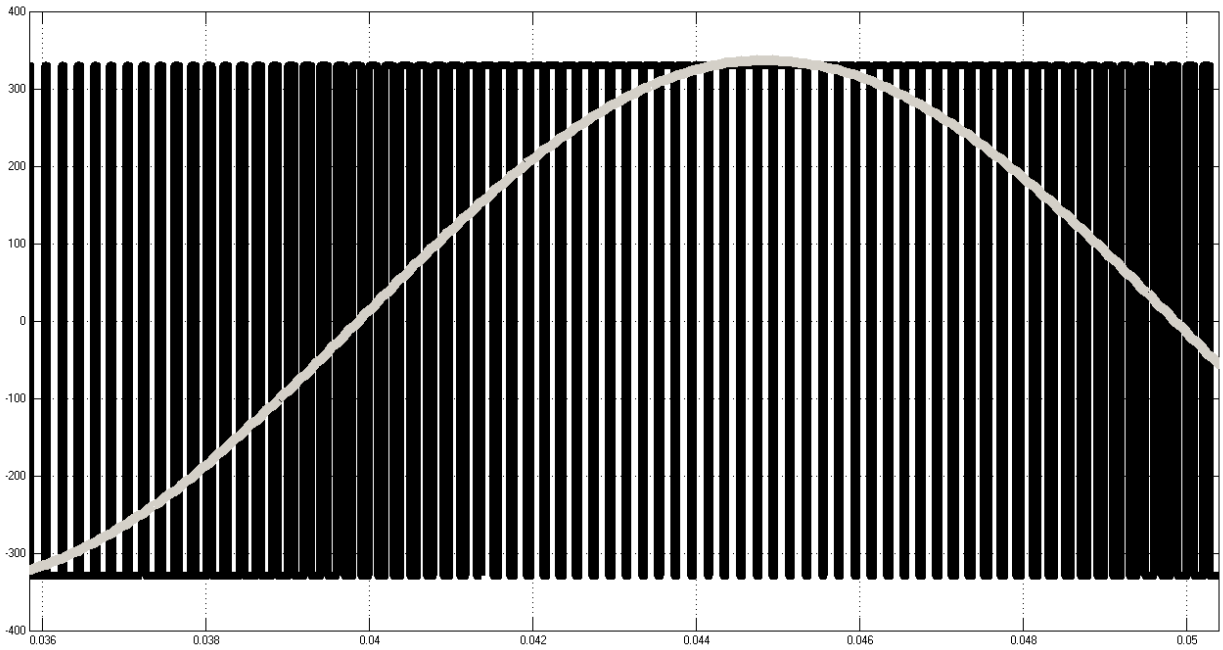


Figure 2.12 Operation Of Single Phase Inverter

### 2.2.3.2 Three-phase Inverters:

The three phase inverters similar to the single phase inverters (Half and full bridge) are shown in the Figure 2.13,

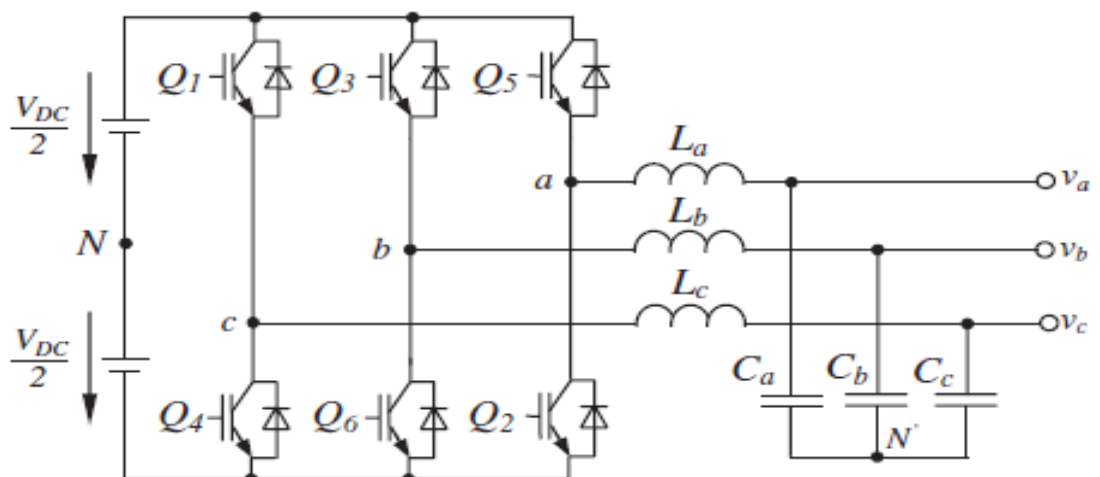


Figure 2.13 Three Phase Inverter

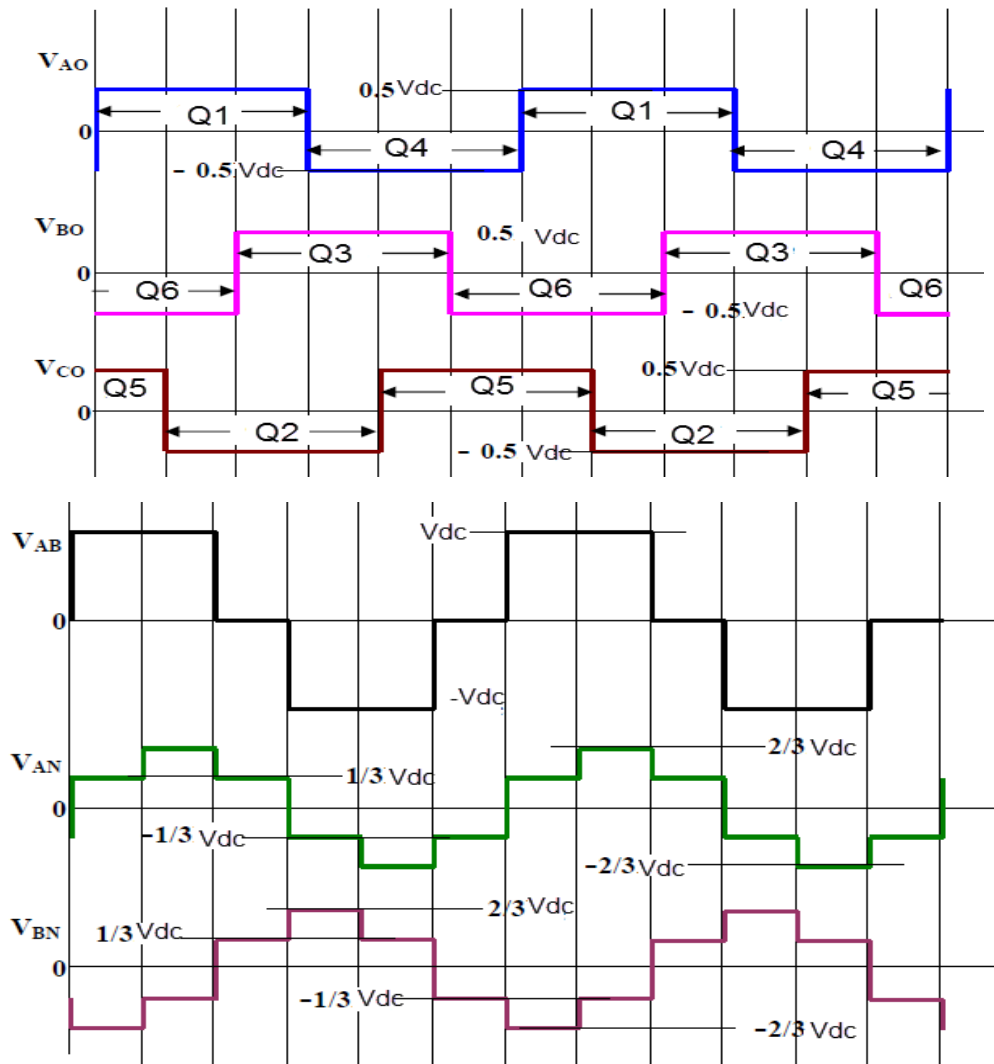


Figure 2.14 Voltage Waveforms Output by a 3-Phase Square Wave

About the indication pattern in Figure 2.14 there are six combinations of conducting switches during an output cycle:-

(Q5,Q6,Q1) , (Q6,Q1,Q2) , (Q1,Q2,Q3) , (Q2,Q3,Q4) , (Q3,Q4,Q5) , (Q4,Q5,Q6). Each of these combinations of switches conducts for  $60^\circ$ , in these sequence mentioned above top reduce output phase sequence of A, B, C. As will be shown later the fundamental component of the three output line-voltages will be balanced. The load side phase voltage wave forms turnout to be somewhat different from the pole voltage waveforms.

### 3.1 Introduction of control systems:

The study and design of automatic Control Systems, a field known as control engineering, has become important in modern technical society. Control systems is a part of our everyday life. The control engineering is a very large field, Control systems are components that are added to other components, to increase functionality, or to meet a set of design criteria. For example: We have a particular electric motor that is supposed to turn at a rate of 40 RPM. To achieve this speed, we must supply 10 Volts to the motor terminals. However, with 10 volts supplied to the motor at rest, it takes 30 seconds for our motor to get up to speed. This is valuable time lost. The increasing demand of energy with robust and reliability requirements, the people toward clean and renewable energy, the technology will be supporting for distributed generation (DG) units by microgrids. And the microgrids which applied on different types of loads and some of sources. [15]

#### 3.1.1 PID Control:

A PID controller is a simple three-term controller used to optimize the response of the system. The letters P, I and D stand for:

**P – Proportional, I – Integral, D – Derivative**, A typical structure of a PID control system is shown in Figure 3.1, where it can be seen that in a PID controller, **the error signal  $e(t)$  is used to generate the proportional, integral, and derivative actions**, with the resulting signals weighted and summed to form the control signal  $u(t)$  applied to the plant model. A mathematical description of the PID controller is the ideal parallel form.

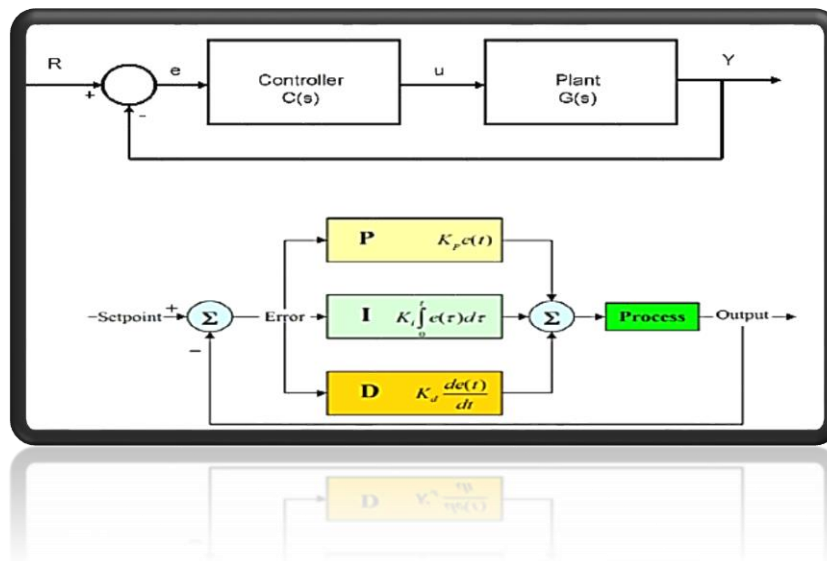


Figure 3.1 Block Diagram of PID Controller

The form of the PID controller most often encountered in industry, and the one most relevant to **tuning algorithms** is the standard form. In this form the  $K_p$  gain is applied to the Integrator, and Differentiator terms, yielding:

$$u(t) = K_p * e(t) + K_t \int_0^t e(t)d(\tau) + K_d \frac{d}{dt} e(t) \dots\dots\dots(3.1)$$

$$u(t) = K_p(e(t) + \frac{1}{T_i} \int_0^t e(t)d(\tau) + T_d \frac{d}{dt} e(t)) \dots\dots\dots(3.2)$$

Where:

**$K_p$  = Proportional Gain**

**$T_i$  = Reset Time, the integral time =  $K_p/K_i$**

**$K_i$ =Integral Gain**

**$T_d$  = Rate or derivative time**

**$K_d$  = Derivative Gain**

**How does the PID parameters affect system dynamics?**

➤ **Proportional gain,  $K_p$**

Larger values typically mean faster response since the larger the error, the larger the proportional term compensation. An excessively large proportional gain will lead to process instability and oscillation.

➤ **Integral gain,  $K_i$**

Larger values imply steady state errors are eliminated more quickly. The trade-off is larger overshoot.

➤ **Derivative gain,  $K_d$**

Larger values decrease overshoot, but slow down transient response and may lead to instability due to signal noise amplification in the differentiation of the error. The behavior of the proportional, integral, and derivative actions will be demonstrated individually through the following example.

**Example:** Consider a third-order plant model given by  $G(s) = 1/(s + 1)^3$ . If a proportional control strategy is selected, i.e.,  $T_i \rightarrow \infty$  and  $T_d \rightarrow 0$  in the PID control strategy, for different values of  $K_p$ , the closed-loop responses of the system can be obtained using the following MATLAB statements, and the result as shown in the Figure 3.2

```
G=tf(1,[1,3,3,1]);
for Kp=[0.1:0.1:1], G_c=feedback(Kp*G,1);
step(G_c), hold on;
End
figure; rlocus(G,[0,15])
```

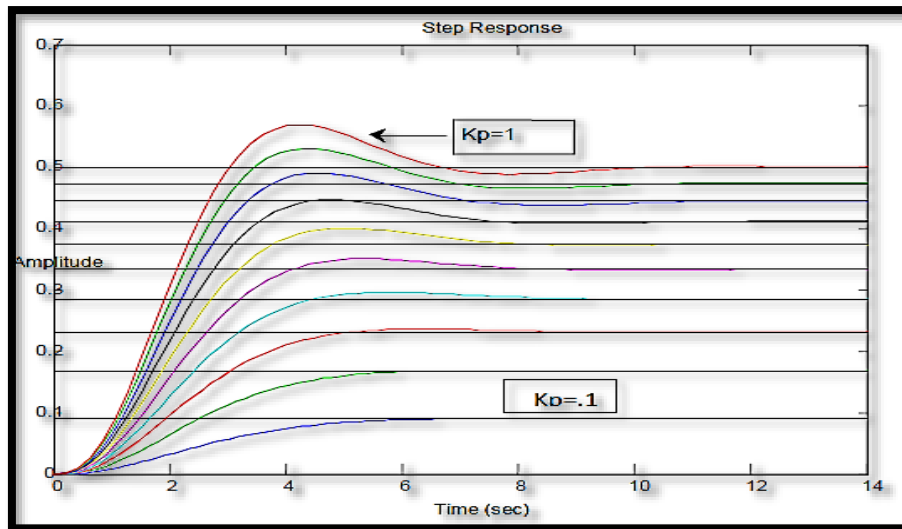


**Figure 3.2(a)** Step Response of Kp Controller

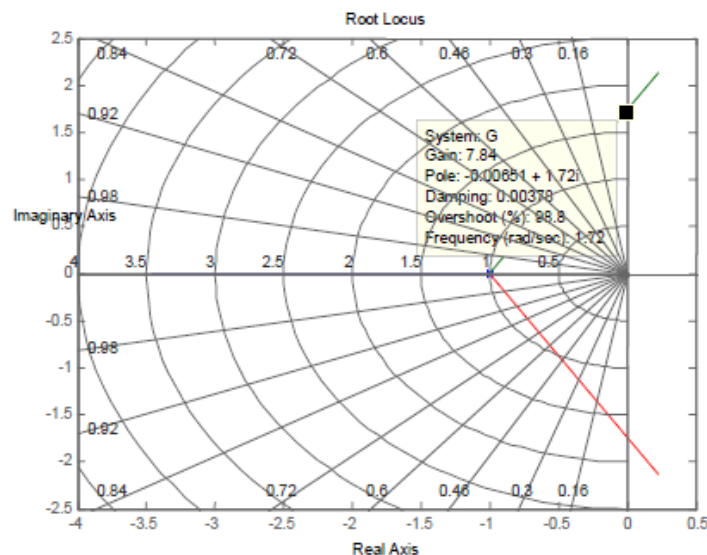


**Figure 3.2(b)** Root Locus of Kp Controller

The closed-loop step responses are obtained as shown in Figure 3.2(a), and it can be seen that when  $K_p$  increases, the response speed of the system increases, the overshoot of the closed-loop system increases, and the steady-state error decreases. However when  $K_p$  is large enough, the closed-loop system becomes unstable, which can be directly concluded from the root locus analysis. The root locus of the example system is shown in Figure 3.2(b), where it is seen that when  $K_p$  is outside the range of  $(0, 8)$ , the closed-loop system becomes unstable.

**If we fixed  $K_p = 1$  and apply a PI (proportional plus integral) control strategy for different values of  $T_i$ , we can use the following MATLAB statements:**

```
>> Kp=1; s=tf('s');
forTi=[0.7:0.1:1.5]
Gc=Kp*(1+1/Ti/s); G_c= feedback(G*Gc,1);
step(G_c), hold on
end
```

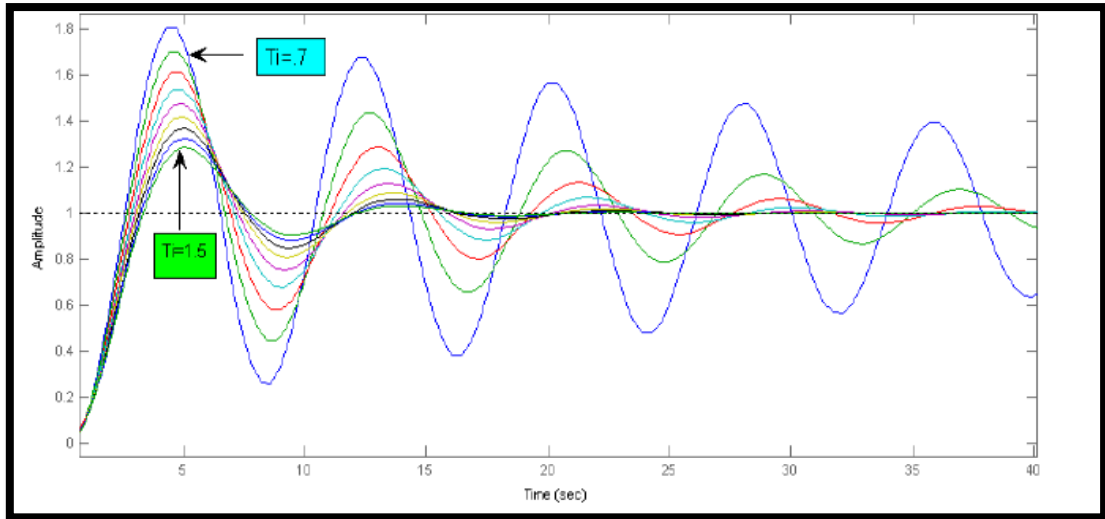


**Figure 3.3** Step Response of PI Controller

To generate the closed-loop step responses of the example system shown in Figure 3.3, the most important feature of a PI controller is that there is no steady-state error in the step response if the closed-loop system is stable. Further examination shows that if  $T_i$  is smaller than 0.6, the closed-loop system will not be stable. It can be seen that when  $T_i$  increases, the overshoot tends to be smaller, but the speed of response tends to be slower.

**Fixing both  $K_p$  and  $T_i$  at 1, i.e.,  $T_i = K_p = 1$ , when the PID control strategy is used, with different  $T_d$ , we can use the MATLAB statements:**

```
Kp=1; Ti=1; s=tf('s'); for Td=[0.1:0.2:2]
Gc=Kp*(1+1/Ti/s+Td*s);
G_c=feedback(G*Gc,1); step(G_c), hold on
end
```

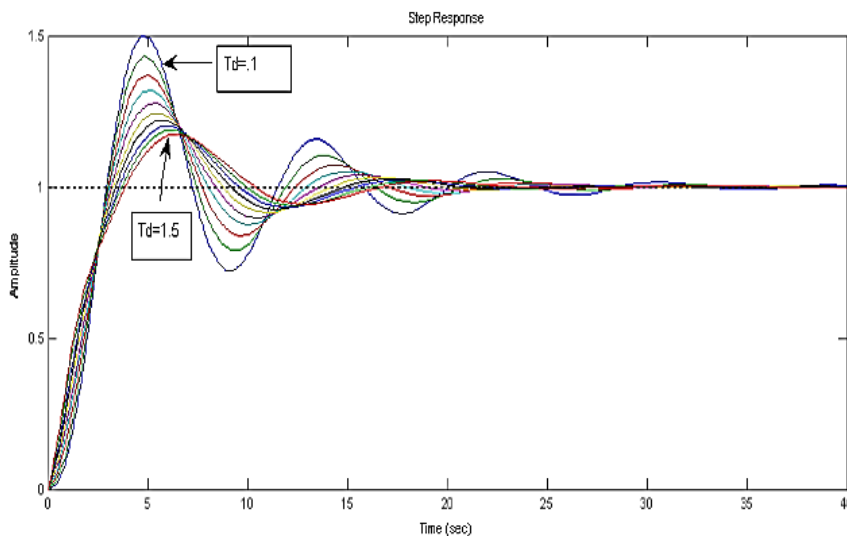


**Figure 3.4** Step Response of PID Controller



When  $T_d$  increases the response has a **smaller overshoot** with a **slightly slower rise time** but **similar settling time**, as shown in the Figure 3.4

### 3.1.1.1 Tuning PID controller:

Here is a table summarize the techniques:

*Table 3.1 Summarize The PID Techniques*

Choosing a Tuning Method		
Method	Advantages	Disadvantages
Manual Tuning	No math required.	Requires experienced personnel.
Ziegler-Nichols	Proven Method.	Process upset, some trial-and-error, very aggressive tuning.
Software Tools	Consistent tuning. May include valve and sensor analysis. Allow simulation before downloading. Can support Non-Steady State (NSS) Tuning.	Some cost and training involved.
Cohen-Coon	Good process models.	Some math. Only good for first-order processes.

### 3.1.1.2 Ziegler-Nichols Tuning:

#### I. First method

This method is applied to plants with step responses of the form displayed in Figure 3.5, This type of response is typical of a first order system .It is also typical of a plant made up of a series of first order systems. The response is characterized by two parameters,  $L$  the delay time and  $T$  the time constant. These are found by drawing a tangent to the step response at its point of inflection and noting its intersections with the time axis and the steady state value. The plant model is therefore. [16]

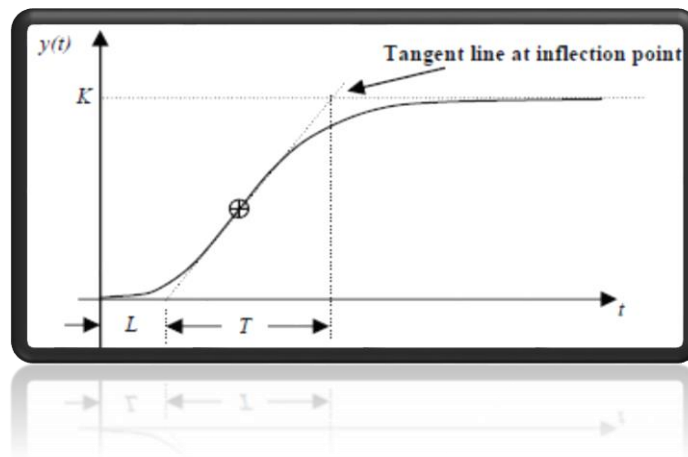


**Figure 3.5** Response Curve for Ziegler-Nichols (First Method)

**Table 3.2** Tuning of PID Controller Parameter According to Z-N Tuning

PID Type	$K_p$	$T_i=K_p/K_i$	$T_d=K_d/K_p$
P	$\frac{T}{L}$	$\infty$	0
PI	$0.9\frac{T}{L}$	$\frac{L}{0.3}$	0
PID	$1.2\frac{T}{L}$	$2L$	$0.5L$

## II. Second method

Using only proportional feedback control:

1. Reduce the integrator and derivative gains to 0.
2. Increase  $K_p$  from 0 to some critical value  $K_{pc}=K_{cr}$  at which sustained oscillations occur.
3. Note the value  $K_{cr}$  and the corresponding period of sustained oscillation,  $P_{cr}$ .

The controller gains are now specified as follows:

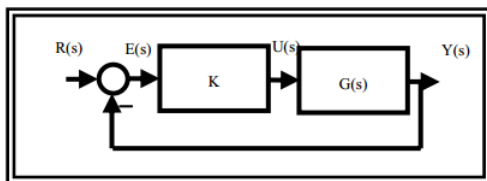
**Table 3.3** Tuning of PID Controller Parameter According to Second Z-N Tuning

PID Type	$K_p$	$T_i$	$T_d$
P	$0.5 K_{cr}$	$\infty$	0
PI	$0.45 K_{cr}$	$\frac{P_{cr}}{1.2}$	0
PID	$0.6 K_{cr}$	$\frac{P_{cr}}{2}$	$\frac{P_{cr}}{8}$

### Example:

The plant is given in transfer function mode such that:

$$G(s) = \frac{1}{(s+1)(s+3)(s+5)}$$



$$\left. \begin{aligned} 1 + KG(s) &= 0 \Leftrightarrow \\ (s+1)(s+3)(s+5) + K &= 0 \Leftrightarrow \\ p(s) = s^3 + 9s^2 + 23s + 15 + K &= 0 \end{aligned} \right\}$$

The corresponding Routh array is

$$\begin{array}{cccc} s^3 & 1 & 23 & 0 \\ s^2 & 9 & 15 + K & 0 \\ s^1 & 192 - K & 0 & \\ s^0 & 15 + K & & \end{array}$$

From this we see that the range of  $K$  for stability is  $15+K>0 \Rightarrow K>-15$  and  $192-K>0 \Rightarrow K<192$ . So  $K_{cr}=192$ . When  $K = 192$ , we have imaginary roots since the  $s^1$  row is identically 0. The corresponding auxiliary equation is

$$9s^2+15+192=0$$

with roots at  $s = \pm j4.8$ . Since this is a quadratic factor of the characteristic polynomial  $\Rightarrow$  the sustained oscillation at the limiting value of  $K$ ,  $K_{cr}$ , is at  $4.8\text{rad/s}$ . Thus,  $P_{cr} = 1.31\text{sec}$  and  $K_{cr} = 192$ . This gives for full PID control from the table as  $K_p = 0.6K_{cr} = 115.2$ ;  $K_i = 2K_p/P_{cr} = 177.2$  ;  $K_d = K_p T_d = K_p/8 P_{cr} = 18.3$ .

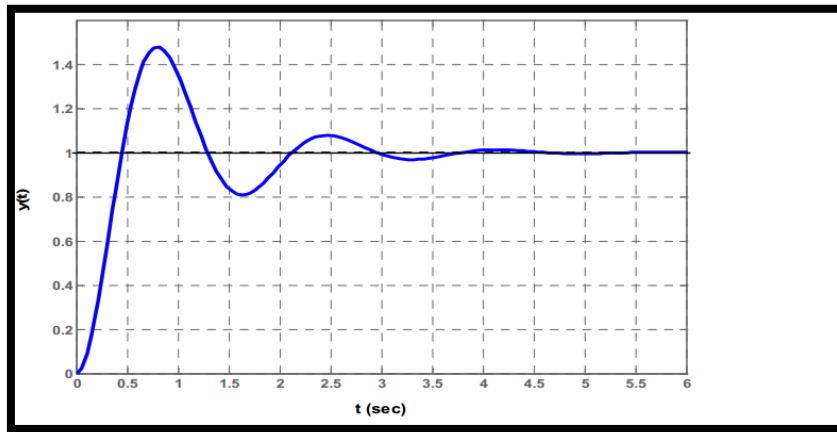


Figure 3.6 Step Response for System Tuned Via the Second Method

## 3.2 Microgrid Literature:

### 3.2.1 Voltage and Current Regulation:

The goals of this technique a power flow for voltage stability improvement in microgrid, low distortion, and regulated in voltage. The proposed control scheme has been developed to control real power (P) or reactive power (Q) by PI and PID controllers, adaptive controllers, and repetitive controllers.

### 3.2.2 Power and Energy management:

Storage energy management are the functionalities expected for these small grids. This way, the energy can be generated and stored near the consumption points, thus increasing of liability and reducing the losses produced by the large power lines. In this technique, the main concepts related to the configuration, control, and energy management of intelligent microgrids are reviewed [17], and proposed solution by Hierarchical Control of Microgrids.

#### ➤ Hierarchical Control of Microgrids:

Functionally, the microgrid, in a similar way as the main grid, can operate by using the following three main hierarchical control levels (see Figure 3.7):

1. Primary control is the droop control used to share load between converters.
2. Secondary control is responsible for removing any steady-state error introduced by the droop control.
3. Tertiary control concerning more global responsibilities decides the import or export of energy for the microgrid.

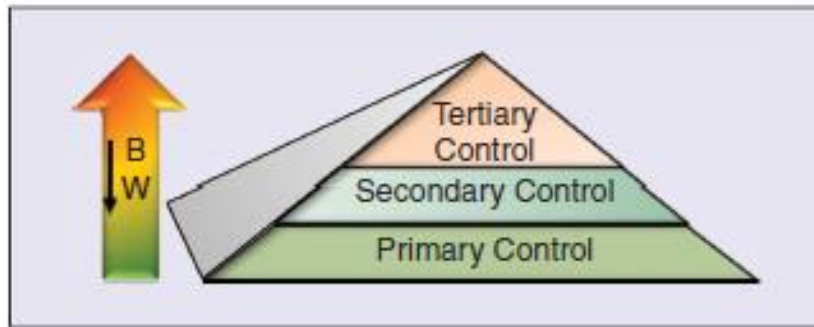


**Figure 3.7** Hierarchical Operation Modes of the Flexible Microgrid

### 3.2.3 Power Sharing:

The distributed generators (DG) with multiple inverters is regulated by controllable frequency and the voltage deviation from the nominal value due to the loss power transfer from main grid and island grid, without communication between the inverters, as shown in Figure 3.8,

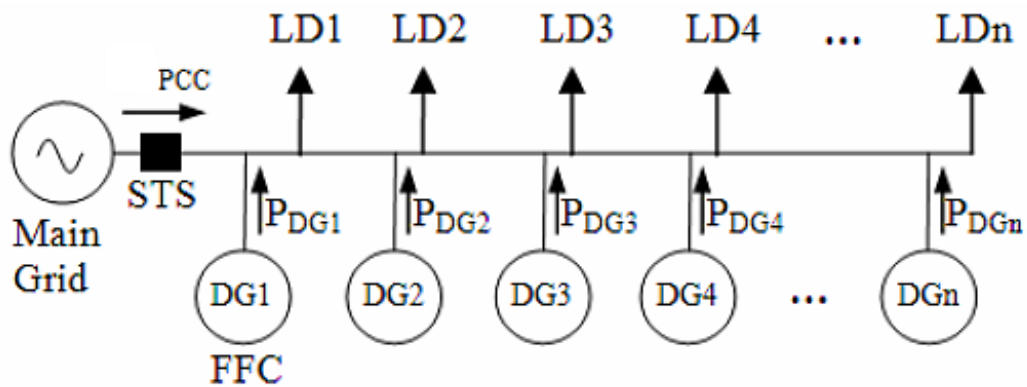


**Figure 3.8** Simplified Grid Connected Microgrid With Multiple Distributed Generators

The proposed solution of power sharing by master-slave controllers and current chain schematic, or Droop controllers will be discussed in this research and used as a controller to improve the active power and reactive power sharing to load demand. There are many techniques to parallel inverters which are already suggested in the literature and will be discussed in the following subsections.

### 3.2.3.1 Master/slave control techniques:

The master/slave control method uses a voltage-controlled inverter as a master unit and current-controlled inverters as the slave units. The master unit maintains the output voltage sinusoidal, and generates proper current commands for the slave units [18-20]. (See Figure 3.9)

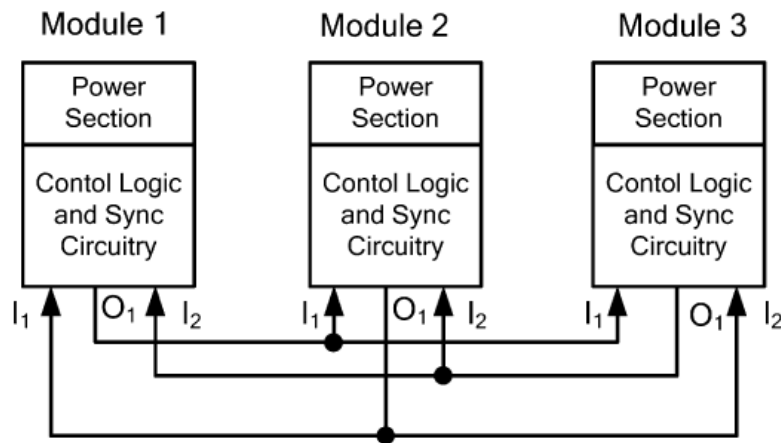


Figure 3.9 Master/Slave Configuration

### 3.2.3.2 Current/power sharing control techniques:

In this control technique the total load current is measured and divided by the number of units in the system to obtain the average unit current. The actual current from each unit is measured and the difference from the average value is calculated to generate the control signal for the load sharing [21].

### 3.2.3.3 Frequency and voltage droop control techniques

There are many methods in this field, Author in [22] used a control technique for operating two or more single phase inverters in parallel connection, as shown in Figure 3.10, This technique is similar to the conventional frequency/voltage droop concept using frequency and fundamental voltage droop to allow all independent inverters to share the load in proportion to their capacities.

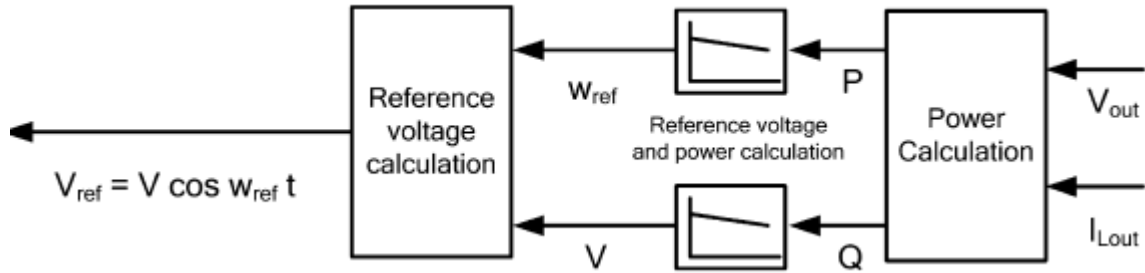


Figure 3.10 Reference Voltage and Power Calculation

By droop control equations are used to control the inverters are working in parallel a constant voltage and frequency system, with no communication between the inverters. (See Figure 3.11)

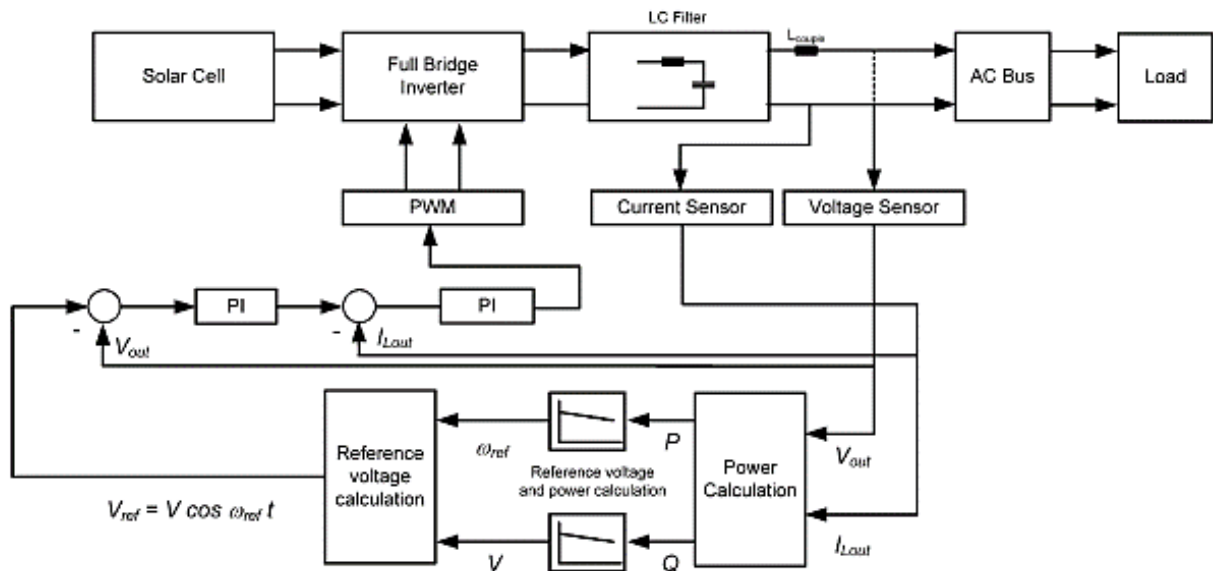


Figure 3.11 Inverter Control Scheme with Droop Control

### 3.3 Particle Swarm Optimization:

Particle swarm optimization (PSO) was originally designed and introduced by Eberhart and Kennedy , 1995. PSO is basically developed through simulation of bird flocking in two-dimension space. The position of each agent is represented by XY axis position and also the velocity is expressed by vx (the velocity of X axis) and vy (the velocity of Y axis). Modification of the agent position is realized by the position and velocity information.

- Each agent knows its best value so far (pbest) and its XY position.
- each agent knows the best value so far in the group (gbest) among pbests.
- Each agent tries to modify its position using the following information:

- the current positions (x, y),
- the current velocities (vx, vy),
- the distance between the current position and pbest.
- the distance between the current position and gbest.

Figure 3.12 shows a concept of modification of a searching point by PSO and Figure 3.13 shows a searching concept with agents in a solution space. Each agent changes its current position using the integration of vectors as shown in Figure 3.12.

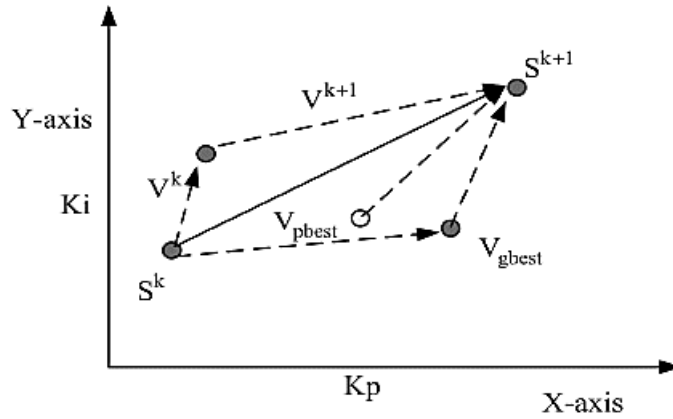


**Figure 3.12** Concept of Modification of Searching Point by PSO.

This modification can be represented by the concept of velocity. Velocity of each agent can be modified by the following equation:

$$V_i^{k+1} = WV_i^k + C_1 \text{rand}_1 \times (\text{pbest}_i - S_i^k) + \dots \\ C_2 \text{rand}_2 \times (\text{gbest} - S_i^k)$$

Where,

$V_i^k$  : Velocity of agent i at iteration k,

W: weighting function,

$C_j$  : weighting factor,

rand: random number between 0 and 1,

$S_i^k$  : Current position of agent i at iteration k,

$\text{pbest}_i$  : pbest of agent i,

gbest: gbest of the group.

Using the above equation, a certain velocity, which gradually gets close to pbest and gbest can be calculated. The current position (searching point in the solution space) can be modified by the following equation:

$$S_i^{k+1} = S_i^k + V_i^{k+1}$$

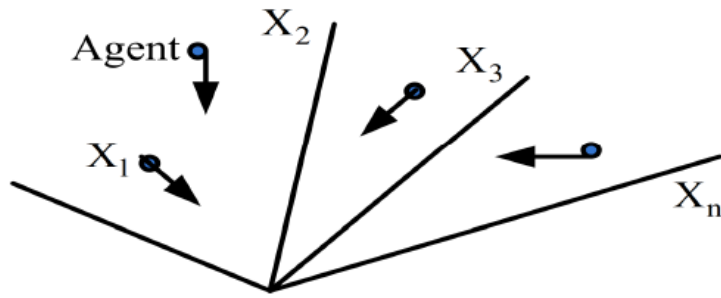


**Figure 3.13** Searching Concepts with Agents in Solution Space by PSO.

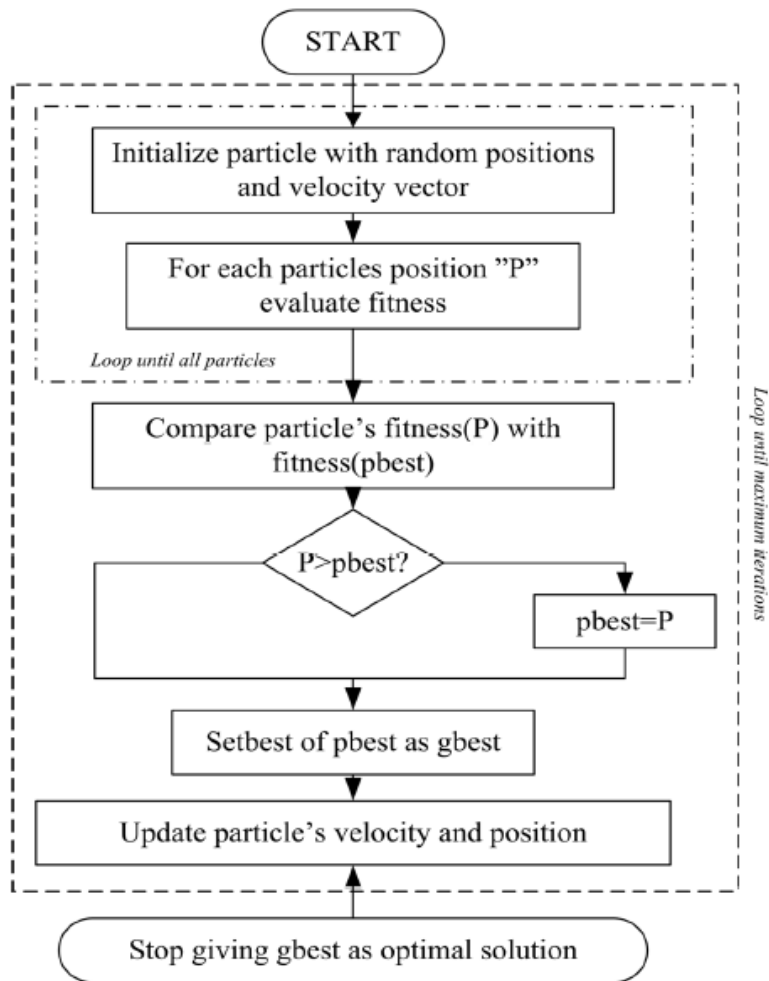


**Figure 3.14** Particle Swarm Optimization Flow Chart



## The Control Inverters for Parallel Operation

### 4.1 Introduction:

Inverters may have to be operated in parallel operation, How to share the power of the load by among inverters operated in parallel, the reasons make an inverters are used to operate in parallel:

1. The limited availability of high current power electronic devices.
2. Make redundancy system, where the parallel inverters are robust and high reliability to stability of the systems.

In this chapter will prove the equations for droop controller to share the loading for two parallel inverters. In the multiple inverters operating in stand-alone mode, each set-point has to be adjusted according to the power rating of the inverter, the power set-point has two different purposes depending on the mode of operation:

- 1) In grid-connected mode, power set-point is set to control the output power.
- 2) In stand-alone mode, it is used to reduce the frequency deviation. Before changing from grid-connected to stand-alone mode the supervisory controller needs to bring all the power set-points of all paralleled inverters to their nominal values before disconnecting from the grid.

### 4.2 Droop Control:

A microgrid consisting of two inverters as shown in Figure4.1, and the reference voltages of the two inverters are following,

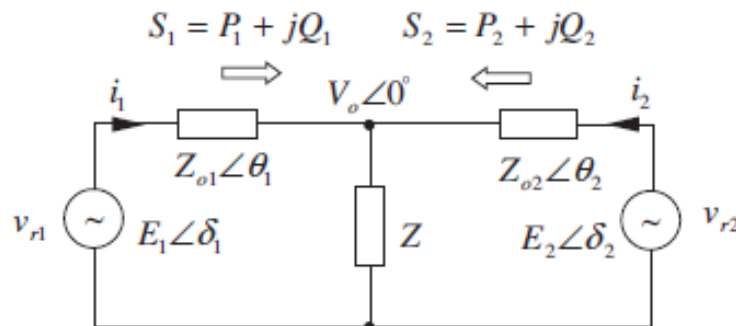


Figure 4.1 Two Inverters Connected in Parallel

$$vr1 = \sqrt{2} E1 \sin(w_1t + \delta_1) \dots\dots\dots (4.1)$$

$$vr2 = \sqrt{2} E2 \sin(w_2t + \delta_2) \dots\dots\dots (4.2)$$

Figure 4.1 shows the equivalent circuit for the two inverters operating in island mode. For simplicity, it is assumed that both inverters have identical output impedance. In a small signal model used to analyze the system's behavior. The model will be developed for two inverters in island mode. As shown in Figure 4.2, the power ratings of the inverters are:

$$S_1 = E_1 I_1^* = P_1 + jQ_1 \dots\dots\dots (4.3)$$

$$S_2 = E_2 I_2^* = P_2 + jQ_2 \dots\dots\dots (4.4)$$

An inverter can be modeled by a two-terminal Thevenin equivalent circuit as shown in Figure 4.2,

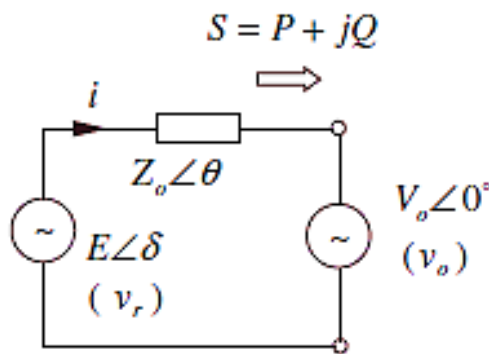


Figure 4.2 Equivalent Model of Voltage Source Inverter

Through an output impedance  $Z_o\angle\theta$  represent output impedance [23].

#### 4.2.1 Power calculation and equations:

The current that flows from each inverter can be described as follows:

$$i_n = \frac{E_n\angle\delta_n - V_o\angle 0}{Z_o\angle\theta} \quad \text{Where } n=1,2 \dots\dots\dots (4.5)$$

Where  $Z_o\angle\theta = R + jX$  is the sum of inverter output impedance and line impedance for the overhead lines, the line impedance mainly exhibits inductive characteristic, that is  $X \gg R$ , and hence  $\theta \approx 90^\circ$ .

$$i_n = \frac{E_n \cos\delta_n + jE_n \sin\delta_n - V_o\angle 0}{Z_o\angle 90} \dots\dots\dots (4.6)$$

Applying Kirchhoff current law at the load node gives: **(the load is  $Z = R$ )**

$$\frac{V_o - E_1\angle\delta_1}{X\angle 90} + \frac{V_o}{R} + \frac{V_o - E_2\angle\delta_2}{X\angle 90} = 0 \dots\dots\dots (4.7)$$

Rearranging (4.7), the load voltage is given by

$$V_o = \frac{R(E_1 \angle \delta_1 - V E_2 \angle \delta_2)}{2R + X \angle 90} \dots\dots\dots (4.8)$$

The real power and reactive power of each inverter via the impedance can then be obtained as

$$P = \left( \frac{E_n V_o}{Z_o} \cos \delta - \frac{V_o^2}{Z_o} \right) \cos \theta + \left( \frac{E_n V_o}{Z_o} \sin \delta \sin \theta \right) \dots\dots\dots (4.9)$$

$$Q = \left( \frac{E_n V_o}{Z_o} \cos \delta - \frac{V_o^2}{Z_o} \right) \sin \theta + \left( \frac{E_n V_o}{Z_o} \sin \delta \cos \theta \right) \dots\dots\dots (4.10)$$

Substituting (4.7) in (4.5) and the result into (4.8), the instantaneous active and reactive powers for the two inverters are given by

$$P_1 = \frac{\left( \frac{X E_1^2}{R} + 2 E_1 E_2 \sin(\delta_1 - \delta_2) \right) + \left( \frac{X E_1 E_2}{R} \cos(\delta_1 - \delta_2) \right)}{4X + \frac{X^3}{R^2}} \dots\dots\dots (4.11)$$

$$Q_1 = \frac{\left( \frac{X^2}{R^2} + 2 \right) E_1^2 - 2 E_1 E_2 \cos(\delta_1 - \delta_2) + \left( \frac{X E_1 E_2}{R} \sin(\delta_1 - \delta_2) \right)}{4X + \frac{X^3}{R^2}} \dots\dots\dots (4.12)$$

$$P_2 = \frac{\left( \frac{X E_2^2}{R} + 2 E_1 E_2 \sin(\delta_2 - \delta_1) \right) + \left( \frac{X E_1 E_2}{R} \cos(\delta_2 - \delta_1) \right)}{4X + \frac{X^3}{R^2}} \dots\dots\dots (4.13)$$

$$Q_2 = \frac{\left( \frac{X^2}{R^2} + 2 \right) E_2^2 - 2 E_1 E_2 \cos(\delta_2 - \delta_1) + \left( \frac{X E_1 E_2}{R} \sin(\delta_2 - \delta_1) \right)}{4X + \frac{X^3}{R^2}} \dots\dots\dots (4.14)$$

Where  $\delta$  the phase difference between the supply and the terminal is, often called the power angle. Where the terminal voltage is  $V_o$ . We can be re-written the real power and reactive power as:

$$P = \frac{E_n V_o}{Z_o} \sin \delta \dots\dots\dots (4.15)$$

$$Q = \frac{E_n V_o}{Z_o} \cos \delta - \frac{V_o^2}{Z_o} \dots\dots\dots (4.16)$$

For the power angle  $\delta$  is closed to zero:

$$\sin \delta \approx \delta \text{ and } \cos \delta = 1$$

Substituting in (4.15) and (4.16), and the result is:

$$P = \frac{E_n V_o}{Z_o} \delta \dots\dots\dots(4.17)$$

$$Q = \frac{E_n - V_o}{Z_o} V_o \dots\dots\dots (4.18)$$

By the derivation, the real power is dependent on the power angle  $\delta$ , and the reactive power depends on the voltage amplitude E. frequency causes dynamic change of the power angle  $\delta$ , the droop control strategies can be obtained of the active power and reactive power by output frequency and voltage amplitude. [24]

As a result of the conventional droop control:

$$\omega_n = \omega^* - K_p P_n \dots\dots\dots(4.19)$$

$$E_n = E^* - K_q Q_n \dots\dots\dots (4.20)$$

When Implementation the droop control practically, the equations in (4.19) and (4.20) after measurement of average values to active and reactive power become:

$$\omega = \omega^* - K_p (P - P^*) \dots\dots\dots(4.21)$$

$$E = E^* - K_q (Q - Q^*) \dots\dots\dots (4.22)$$

Where  $\omega^*$ ,  $E^*$  are the nominal frequency and nominal voltage references,  $K_p$ , and  $K_q$  are the frequency proportional drooping coefficient and voltage proportional drooping coefficient, respectively. The droop slopes are determined according to the power rating of the inverter and according to the maximum allowable variations in output frequency and voltage. This strategy, consisting of the Q – E and P –  $\omega$  droopa, is illustrated in Figure 4.3,

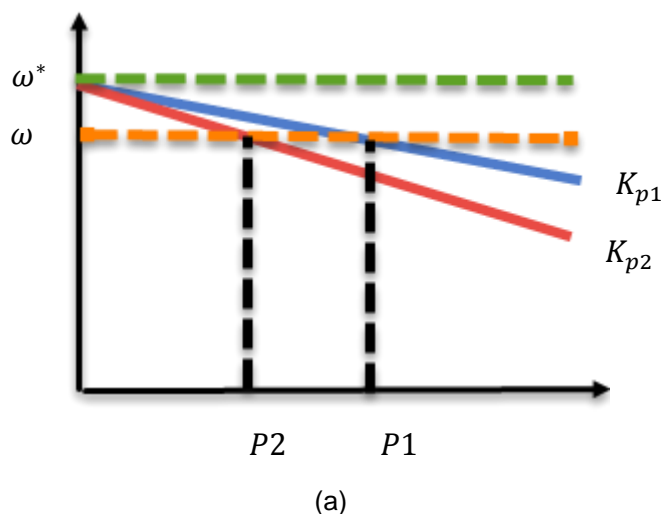
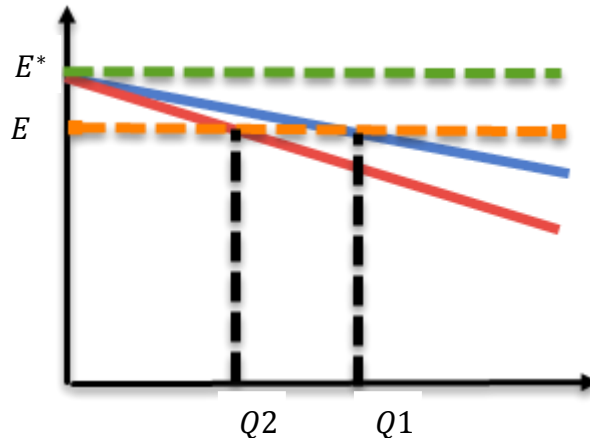


**Figure 4.3(a)** Frequency Droop Control



(b)

**Figure 4.3(b)** Voltage Droop Control

### 4.2.2 Droop control strategy:

The main advantages of P- $\omega$  and Q-E droop control where the inverter frequency and voltage amplitude are drooped linearly with the inverter output active and reactive power, respectively. (P- $\omega$ ) allows parallel connected in a safe way sharing variations in the load without any dedicated communication means. And the (Q-V) droop loop is used to minimize the circulation currents that would appear if the impedance between the inverters.

The power circuit uses a full bridge inverter as shown in Figure 4.4, the inverter output is a high frequency switching waveform.

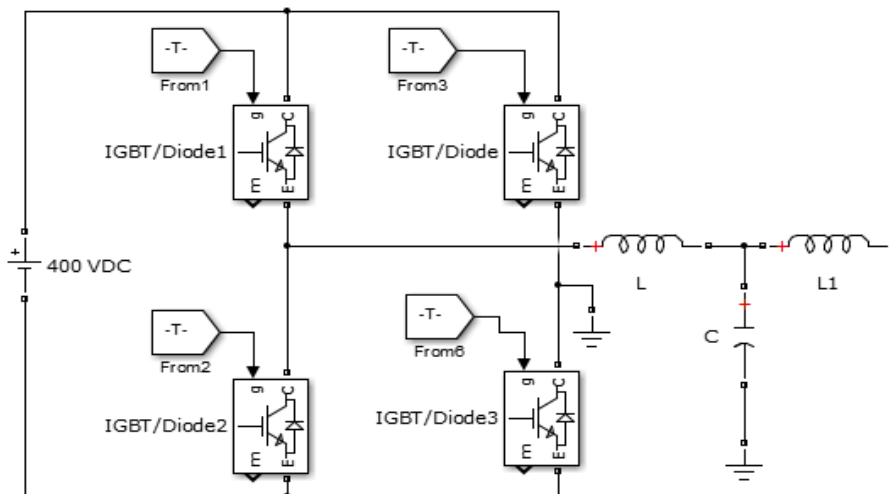


**Figure 4.4** Full Bridge Inverter System.

The parallel structure of two inverter modules is shown in Figure 4.5. Each inverter module uses a full bridge circuit with an LCL filter to restrain high frequency harmonics [25]. A microgrid consisting of two inverters as shown in Figure 4.6 is considered.

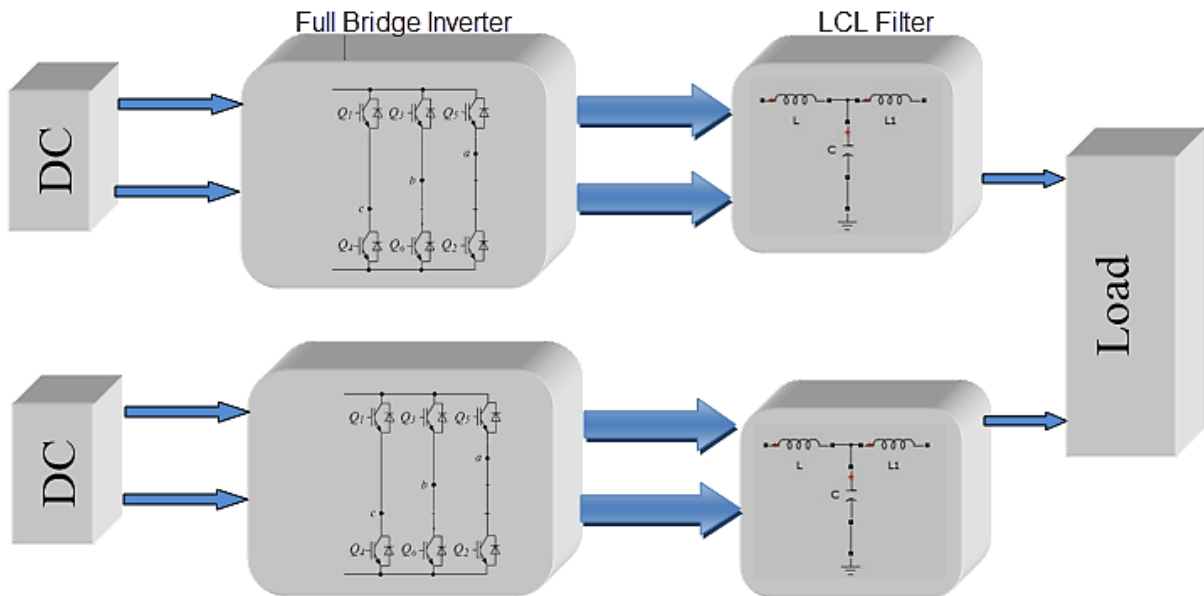


Figure 4.5 Parallel Structure of Two Inverter Modules.

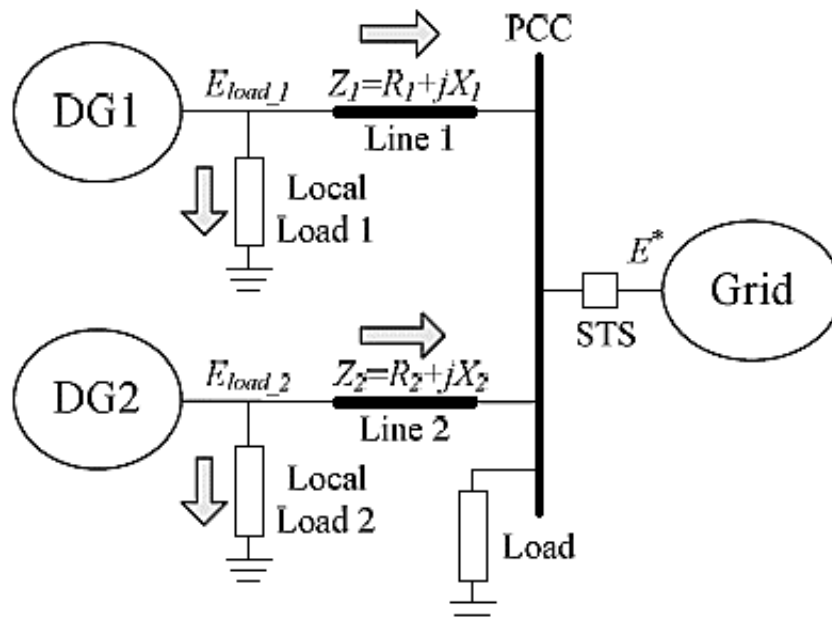


Figure 4.6 Two Inverters in Microgrid.

### 4.2.2.1 Voltage control block:

From the relationship of droop characteristic we can calculate operation frequency  $\omega_{ref}$  and voltage  $V$  of parallel inverters to form reference voltage command  $V_{ref} = E \cos(\omega_{ref}.t)$ . The PI controller is used to compensate voltage error signal  $V_{error}$  and the compensated voltage error signal is to be reference current command  $I_{ref}$ , see Figure 4.7.

### 4.2.2.2 Current control block :

The current control loop is shown in Figure 4.8, Reference current  $I_{ref}$ , subtracts inductance current  $I_L$  to find out error current  $I_{error}$ , then error current command  $I_{error}$ , goes through the PI controller to obtain PWM signal for driving full bridge inverter.

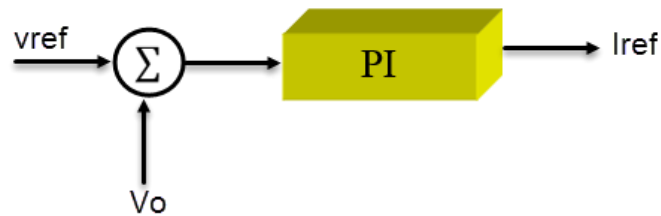


Figure 4.7 Voltage PI Compensator

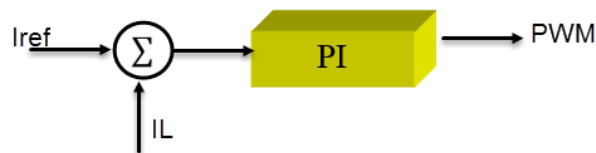


Figure 4.8 Current PI Compensator

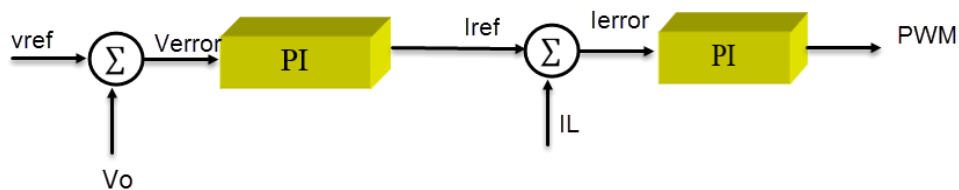


Figure 4.9. Voltage- and Current-Loop Control Structure.

The droop coefficients are selected as follows:

$$K_{p1}S_1 = K_{p2}S_2 = K_{p3}S_3 = \dots \dots \dots K_{pi}S_i \dots \dots \dots (4.23)$$

$$K_{q1}S_1 = K_{q2}S_2 = K_{q3}S_3 = \dots \dots \dots K_{qi}S_i \dots \dots \dots (4.24)$$

Where  $S_1, S_2, S_3, \dots, S_i$  are the apparent power ratings of the inverters.

The total load of the system is  $(P_1 + P_2)$  real power and  $(Q_1 + Q_2)$  reactive power, the reference voltage  $V_{ref} = E \sin(\omega_i t + \delta_i)$  includes two control variables, reference frequency  $\omega_i$  calculated by droop relationship from Eq. (4.21), and voltage  $V$  calculated by droop relationship from Eq. (4.22), as shown in Figure 4.10.

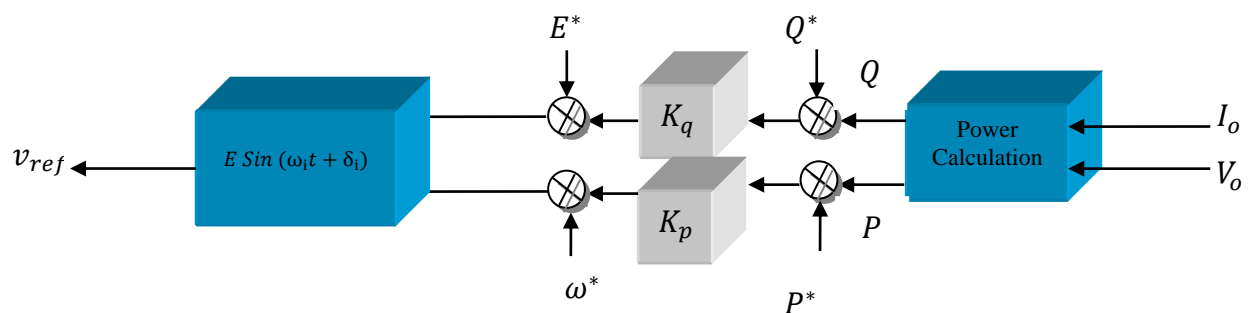


**Figure 4.10** Reference Voltage and Power Calculation

In This research using power proportional distribution between two parallel-connected inverters. Each inverter module control block is shown in Figure 4.11.

### 4.3 SIMULATION RESULTS:

The proposed power control strategy has been verified in Matlab/Simulink simulations. In the simulations, a microgrid with two inverters systems as shown in Figure 4.6 is applied. The simulation parameters of the system are chosen to be the same as shown in Table 4.2. Each DG is interfaced to the microgrid by VSI with LCL filter. The parameters of the filter are listed in Table 4.1. In the simulations, the two DG units are designed with identical parameters to facilitate the observation of the power sharing accuracy.

**Table 4.1** Filtre Parameter Values of The Inverter

Symbol	Description	Value
<b>L1 (uH)</b>	Inverter-side filter inductor	1200
<b>C1 (uF)</b>	Capacitor is used in filter	220
<b>L2 (uH)</b>	Grid-side filter inductor	200





**Table 4.2 Simulation Parameters**

Symbol	Description	Value
$P_1^*$	Nominal Value of Active Power for inverter 1	10K W
$P_2^*$	Nominal Value of Active Power for inverter 2	10K W
$Q_1^*$	Nominal Value of Reactive Power for inverter 1	0 VAR
$Q_2^*$	Nominal Value of Reactive Power for inverter 2	0 VAR
$K_p$	Frequency drooping gain	0.04
$K_q$	Voltage drooping gain	0.01
$E^*$	Nominal Voltage	380 V
$f^*$	Nominal frequency	50 HZ
$\tau$	Measurement filter time constant	0.1 S

The system parameters selected for the calculation of the filter components of the inverter with LCL configuration, we need to provide a sinusoidal voltage, When the carrier frequency, (switching frequency), is high enough, then the harmonic components can be easily filtered out via a low-pass filter, which is often an LC or LCL filter. This type of modulation is called a sinusoidal PWM (SPWM), and the design is shown in Figure 4.12, The SPWM is operated on both legs of the inverter, and the same PWM signal is sent to Q1 and Q2 (two phase legs) in complementary way. The result waves are shown in the Figure 4.13 after and before applying the filter, also, Q3 and Q4 is operated PWM at the same time.

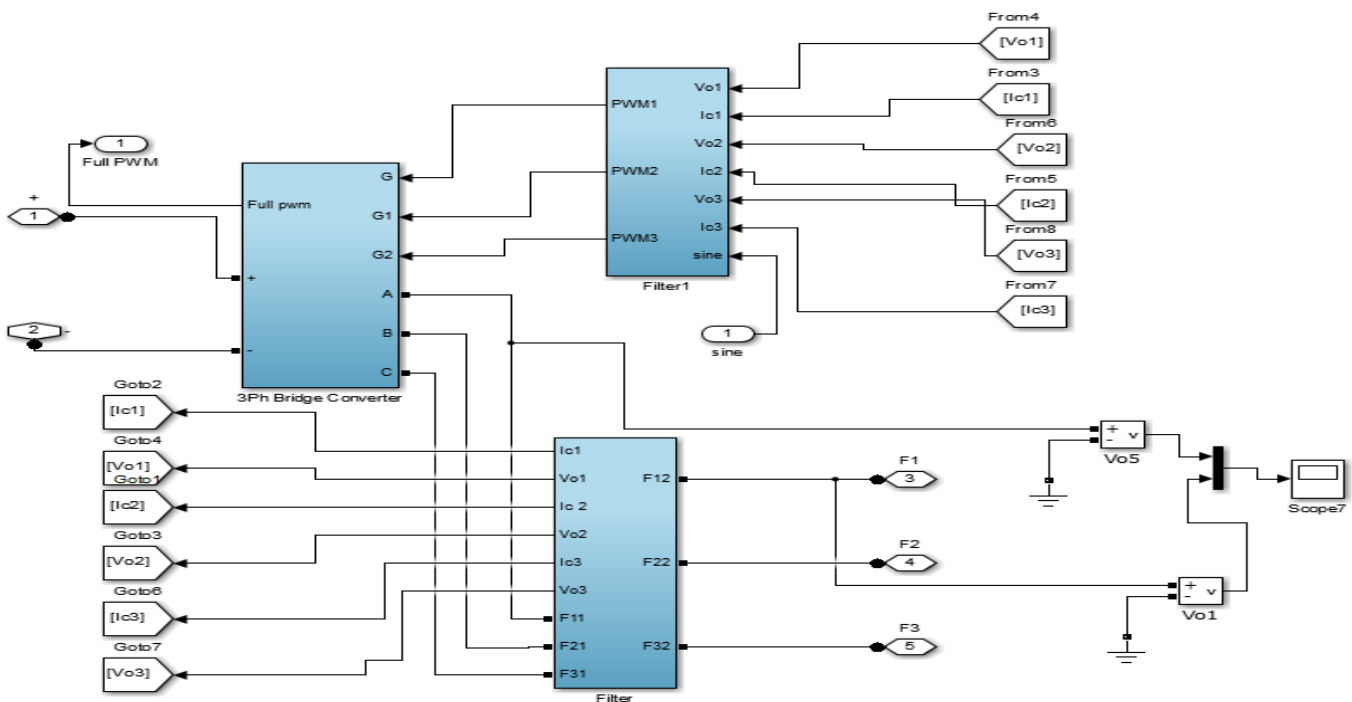


**Figure 4.12 Design sinusoidal inverter**

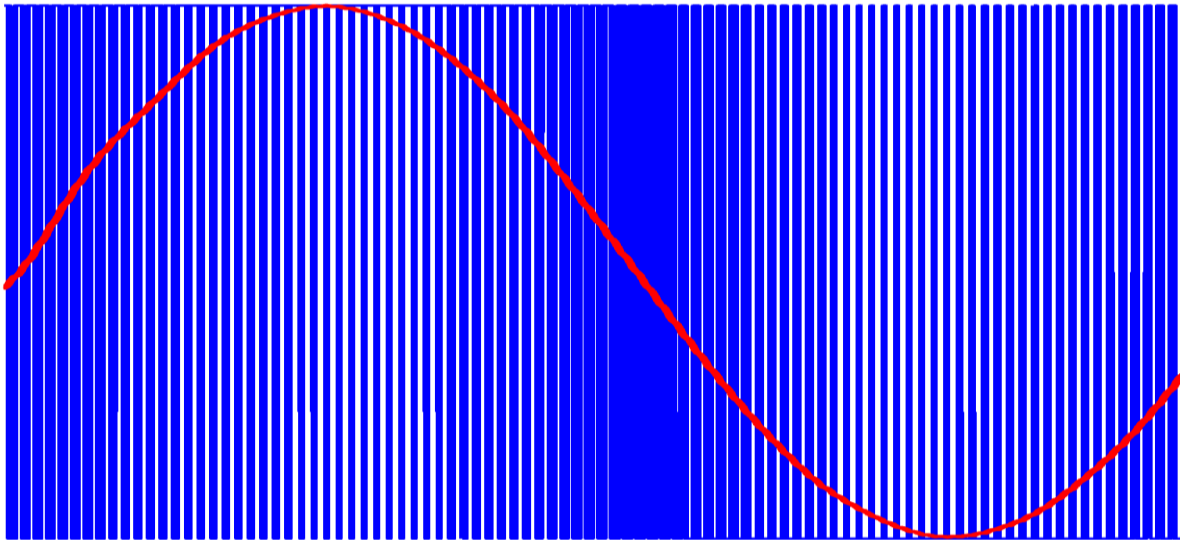


**Figure 4.13** Operation of Single Phase Inverter

With an output rating of 10 KVA, is given in the Table 2. The output phase voltage is shown in Figure 4.12. The load current is shown in Figure 4.13. From Figure 4.12 and Figure 4.13, it is clear that the load current is shared equally between the two inverters. The grid phase voltage obtained is sinusoidal with peak amplitude of 325V at 50 Hz frequency.

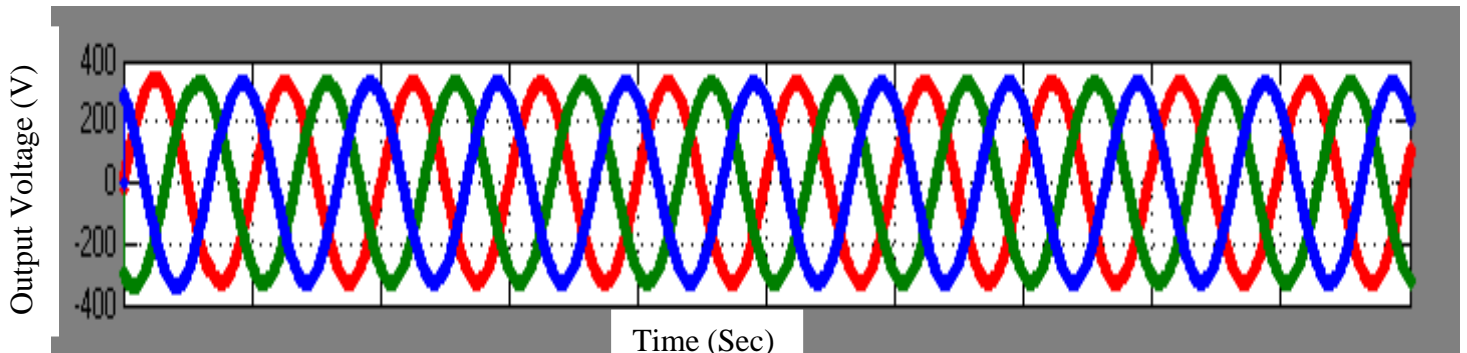


**Figure 4.12** Output Phase Voltage

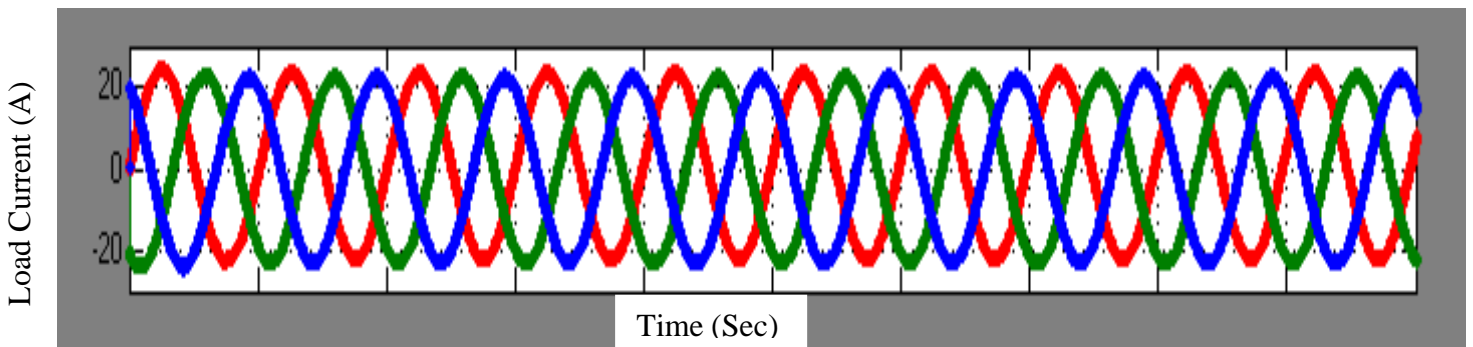


**Figure 4.13** Load Current



### 4.3.1 case I:

Two inverter in island mode with different nominal values, in this case will test the control of power set-points before starting the inverter. In Figure 4.15 display the active power of both inverter with different set- points.

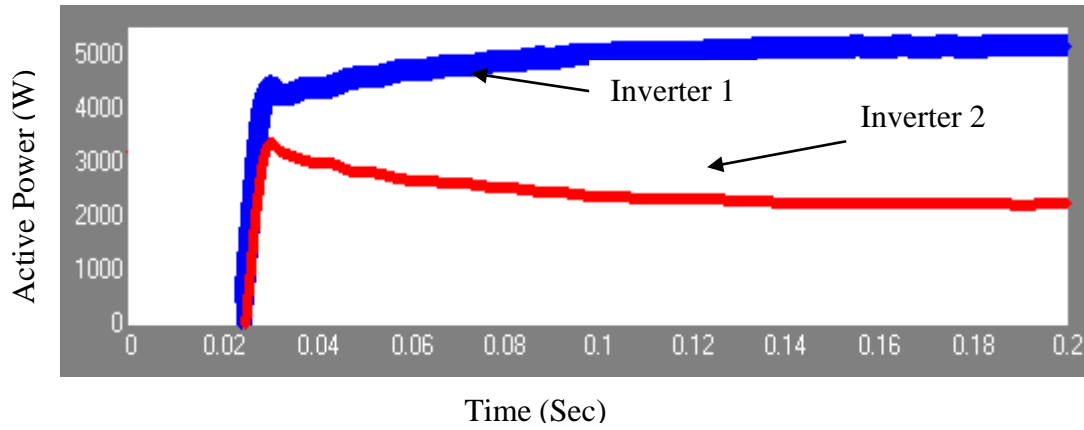


**Figure 4.15** Active Power of Inverters 1 and 2

Similarly, we can see in Figure 4.16, the response of frequency of inverter 1 and inverter 2

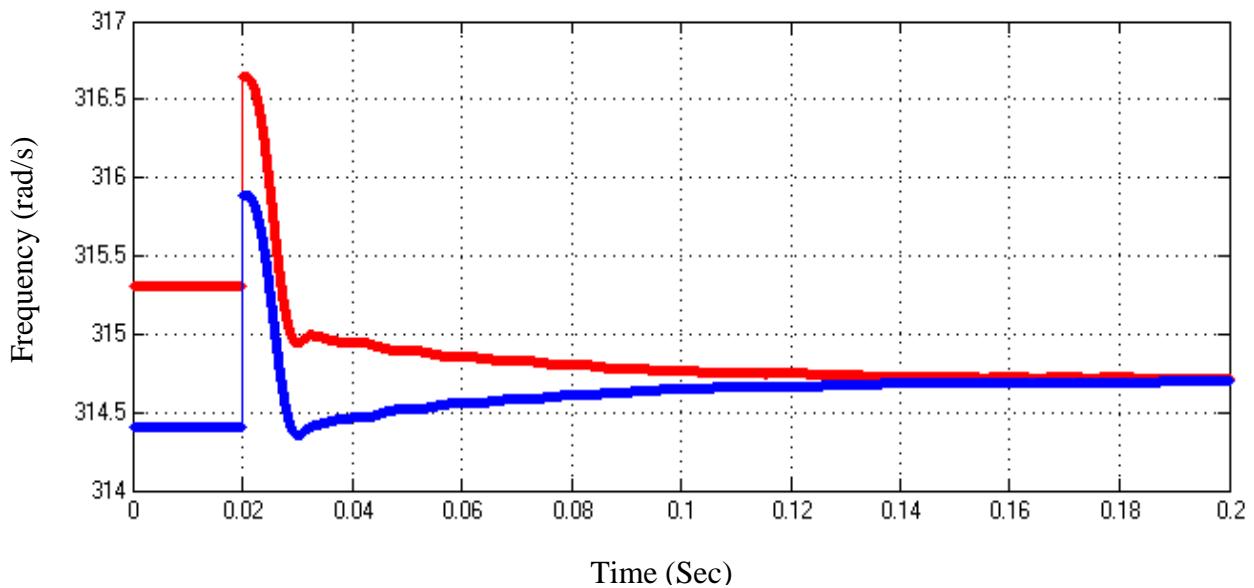
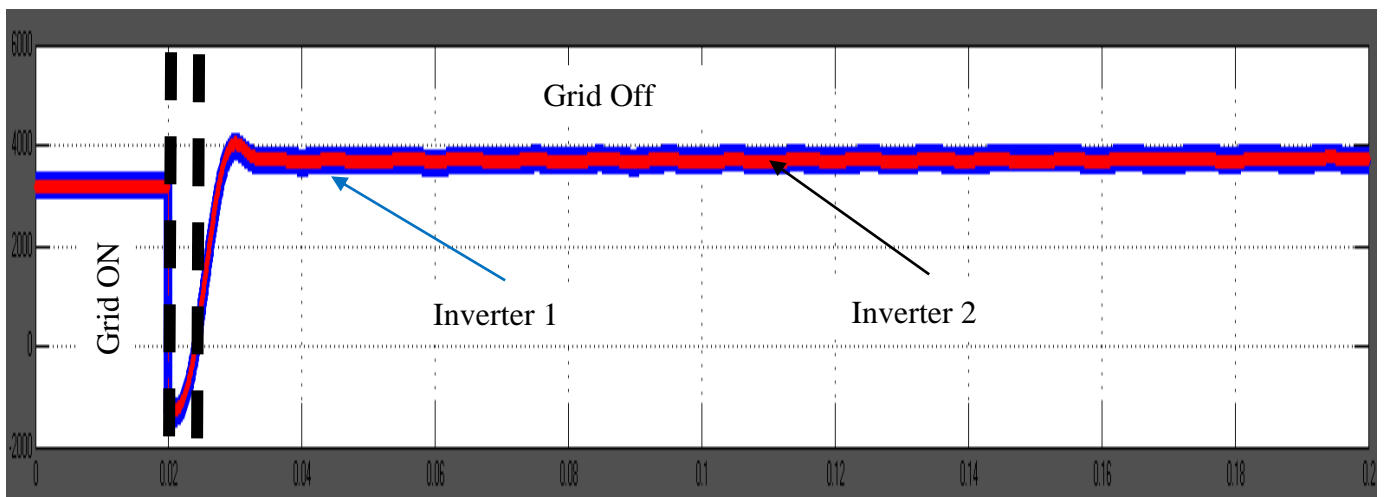


**Figure 4.16** Frequency of Inverters 1 and 2

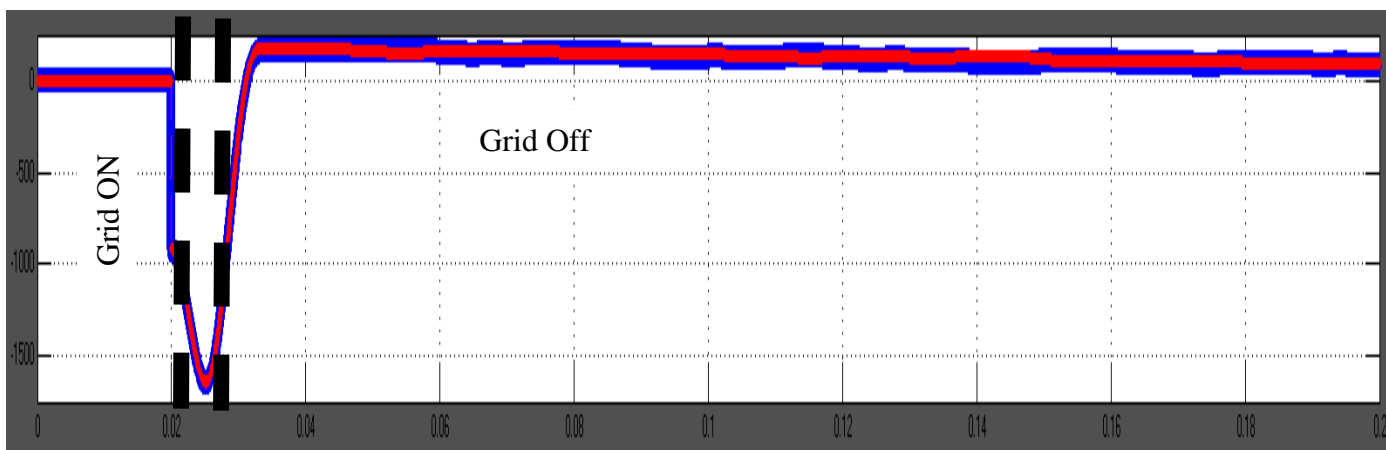
### 4.3.2 case II:

Represents islanding mode when the two inverters have the same set points. In the simulations and experiments, the two DG units are designed with identical parameters to facilitate the observation of the power sharing accuracy. Figure 4.17 shows the real and reactive power flows of the two DG systems in the scenario.

The microgrid system is originally operated in grid-connected mode with dispatched real and reactive power commands of 2700W and 0 Var for each DG system.



(a)



(b)

**Figure 4.17** Power Sharing Performance: (a) Real Power With Traditional Droop Method, (b) Reactive Power With Traditional Droop Method.

At  $t=0.2$  Sec , the microgrid is disconnected from the main grid and operates in islanding mode, and at this moment the two DG units share the total load demand. As shown in Figure. 4.17(a), the real power sharing is accurate. However, as shown in Fig. 4.17(b), with the traditional voltage droop control, where the real power 3800 W , and the reactive power sharing is 105 VAR,

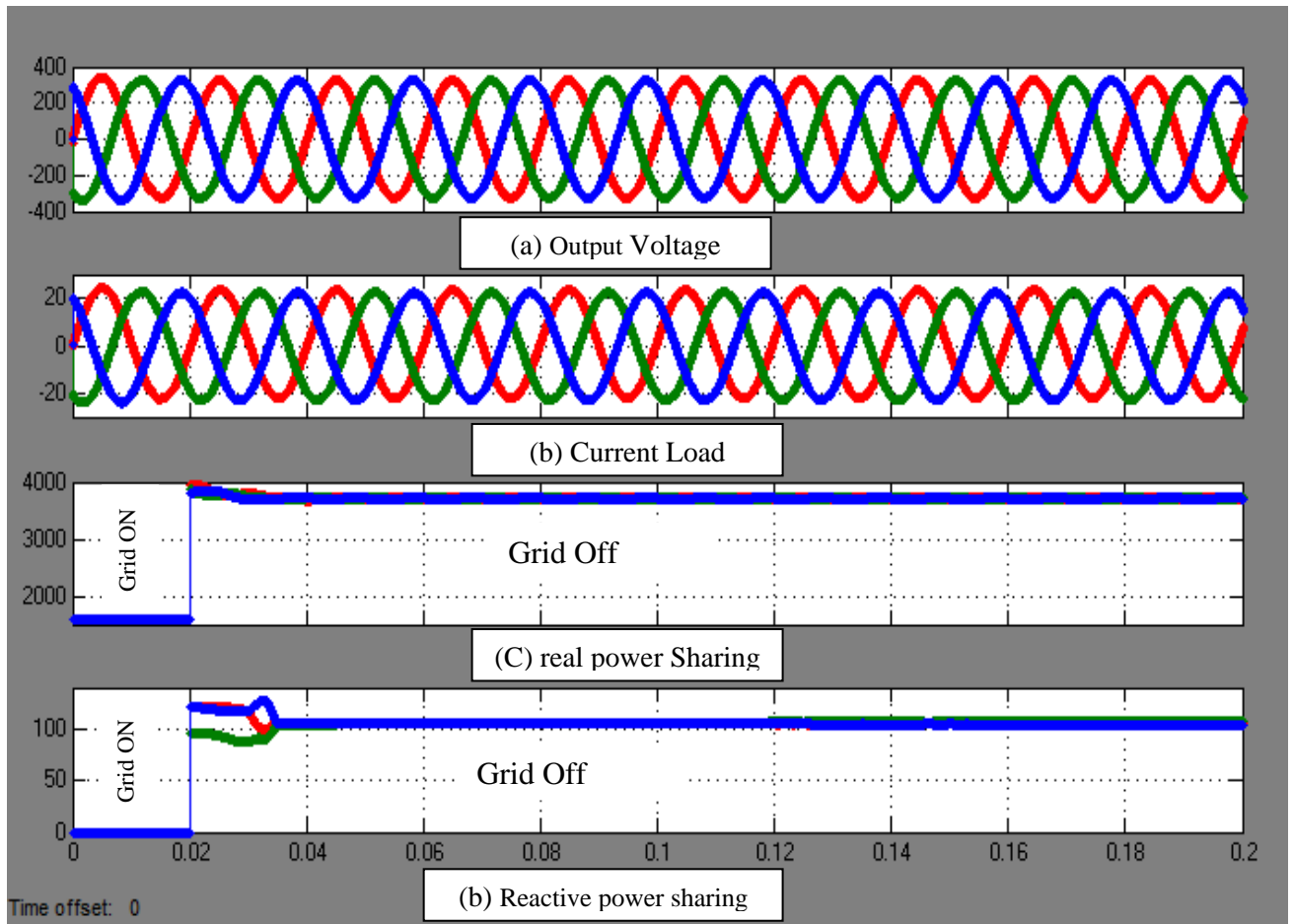


**Figure 4.18** Power Sharing Performance: (a) Accurate Real Power, (b) Reactive Power,

DG systems. Note that the real and reactive power during the islanding transient are caused by the sudden change of voltage magnitude. As expected, when the proposed accurate power sharing algorithm is implemented, as shown in Figure 4.18, the reactive power control has smooth transient and accurate sharing performance as can be seen in the next section.

The main objective of this research is to make accurate real and reactive power sharing. For PSO (Particle swarm optimization) algorithm technique, PID controller is used to improve the performance of microgrid system.

### 4.3.3 Results of PSO:

The performance of PSO is presented in Figure 4.19. It can be seen that the voltages of DG unit1 and DG unit2 are sinusoidal with 0.53% and 0.57% THD (total harmonic distortions), respectively. On the other hand, voltage (with 1.82% THD) is presented in the previous section.

Figure 4.20 shows the real and reactive power flows of the two DG systems in the scenario of no DG local loads and the load at PCC is 4200 W and 1200Var. The microgrid system is originally operated in grid-connected mode with dispatched real and reactive power commands of 1500W and 0Var for each DG system (note that a PID controller is used for the reactive power control as illustrated in Figure 19). At  $t=0.02$  s, the microgrid is disconnected from the main grid and operates in islanding mode. At this moment the two DG units share the total load demand, where the real power and reactive power sharing is accurate, as shown in Figure 4.20.

As expected, when the proposed accurate power sharing algorithm is implemented, the reactive power control has smooth transient and accurate sharing performance as can be seen from figure 4.20(c).

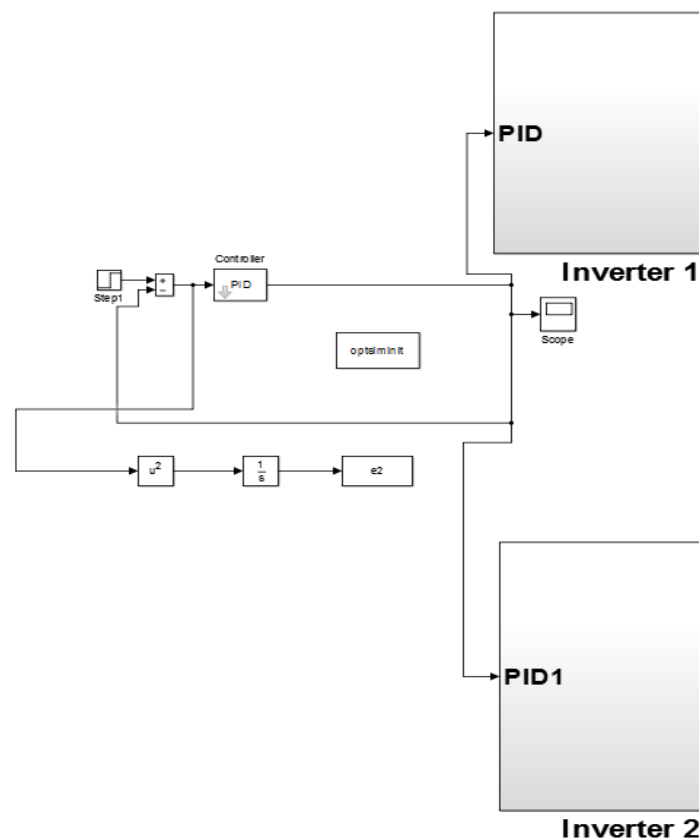


**Figure 4.19** Design Particle Swarm Optimization



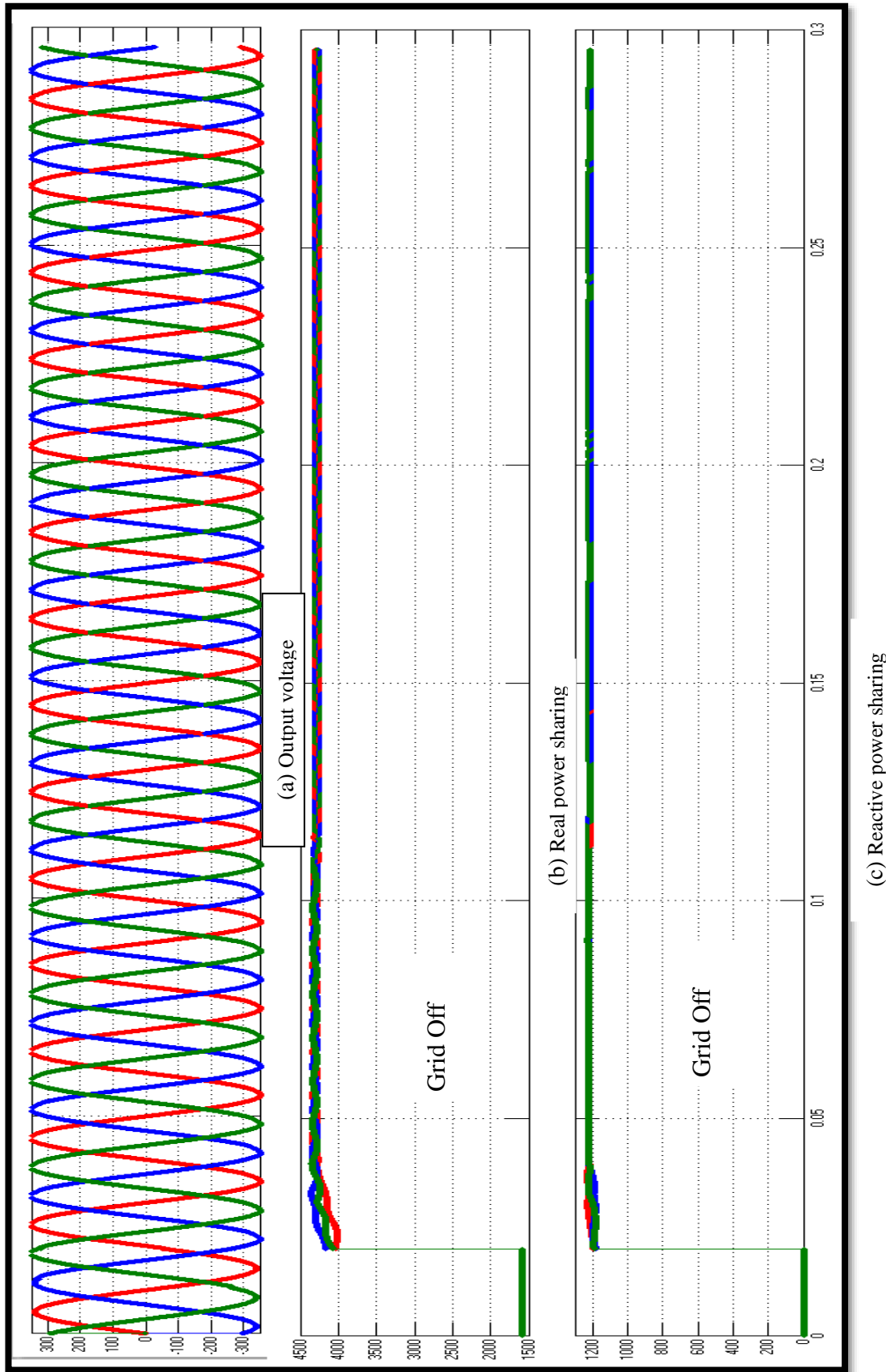


Figure 4.20 Power Sharing Performance with PSO: (a) Accurate Real Power, (b) Accurate Reactive Power

## Conclusion and Future work

### 5.1 Conclusion:

Droop control method is a widely used technique for achieving load sharing in microgrid applications. An improved microgrid reactive power sharing strategy was proposed. This research has investigated the transient power between paralleled inverter during islanding mode and a controller to limit this circulating power has been proposed. And a new optimization procedure is proposed to find the optimal droop parameters such that the effect of deviation in voltage and frequency is minimized. It is confirmed that the parallel inverter can successfully support the islanding operation of the microgrid, The parallel inverter shows good performance in the simulation studies.

### 5.2 Future Work:

Future work could include:

- We will test the microgrid design on a real life to ensure the robustness of this project.
- Integrate infrastructure of classic grid with the fast-paced, disruptive communications and computing technologies that support the smart grid.
- Establishing maintenance free, automated, non-intrusive, real time power monitoring system.
- Measuring performance characteristics of various electrical utilities connected to the grid.
- To promote a sense of responsibility and belonging to every consumer of electricity on campus.
- Extending the idea to develop microgrids for every part of the campus and to integrate them under a single roof –the smart grid.

Microgrids, a cutting-edge technology, feature intelligent control systems that enable self-coordinated operation. With their energy flexibility, cost-efficient scheduling, and optimized management capabilities, they act as controllable power supplies or loads in a power grid network, giving them enormous growth potential.

# REFERENCES:

- [1] Current distribution control design for paralleled DC/DC converters using sliding-mode control Lopez, M.; de Vicuna, L.G.; Castilla, M.; Gaya, P.; Lopez, O. *Industrial Electronics, IEEE Transactions on* Year: 2004, Volume: 51, Issue: 2 Pages: 419 - 428, DOI: 10.1109/TIE.2004.825273.
- [2] Control of Distributed Uninterruptible Power Supply Systems Guerrero, J.M.; Lijun Hang; Uceda, J. *Industrial Electronics, IEEE Transactions on* Year: 2008, Volume: 55, Issue: 8 Pages: 2845 - 2859, DOI: 10.1109/TIE.2008.924173
- [3] K.D. Brabandre, B. Bolsens, J.V.D. Keybus A. Woyte, J. Drisen and R. Belmans , A oltage and frequency droop control method for parallel inverters, *IEEE Trans. Power Electron.*, vol. 22, no. 4, pp. 1107-1115, Jul.2007.
- [4] J. M. Guerrero, L. G. Vicuna, J. Matas, M. Castilla, and J. Miret, Output impedance design of parallel-connected UPS inverters with wireless load sharing control, *IEEE Trans. Ind. Electron.*, vol. 52, no. 4, pp. 1126–1135, Aug. 2005.
- [5] C.-C. Hua, K.-A. Liao, and J.-R. Lin, "Parallel operation of inverters for distributed photovoltaic power supply system," in *IEEE 33rd Annual Power Electronics Specialists Conference*, 2002, pp. 1979-1983.
- [6] Control of parallel connected inverters in standalone AC supply systems Chandorkar , M.C.; Divan, D.M.; Adapa, R. *Industry Applications, IEEE Transactions on* Year: 1993, Volume: 29, Issue: 1 Pages: 136 - 143, DOI: 10.1109/28.195899
- [7] A New Quick-Response and High-Efficiency Control Strategy of an Induction Motor Takahashi , I.; Noguchi, T. *Industry Applications, IEEE Transactions on* Year: 1986, Volume: IA-22, Issue: 5 Pages: 820 - 827, DOI: 10.1109/TIA.1986.4504799
- [8] Control of distributed UPS systems Chandorkar, M.C.; Divan, D.M.; Banerjee, B. *Power Electronics Specialists Conference, PESC '94 Record., 25th Annual IEEE Year: 1994* Pages: 197 - 204 vol.1, DOI: 10.1109/PESC.1994.349730.
- [9] S.H. Hauck Matthias, Wechselrichter problemlos parallel betreiben *Elektronik* H.12/2000, 2000, pp. 120–124.
- [10] Autonomous load sharing of voltage source converters Sao, C.K.; Lehn, P.W. *Power Delivery, IEEE Transactions on* Year: 2005, Volume: 20, Issue: 2 Pages: 1009 - 1016, DOI: 10.1109/TPWRD.2004.838638.
- [11] Rashid M 1993 *Power Electronics: Circuits, Devices and Applications* 2nd edn. Prentice-Hall International.

- [12] Rashid M 2010 Power Electronics Handbook: Devices, Circuits, and Applications Academic Press. Elsevier.
- [13] QingChang\_Zhong,\_Tomas\_Hornik(auth.) 2012, CONTROL OF POWER INVERTERS IN RENEWABLE ENERGY AND SMART GRID INTEGRATION.
- [14] Daniel W. Hart, Power Electronics 2010.
- [15] [http://en.wikibooks.org/wiki/Control\\_Systems](http://en.wikibooks.org/wiki/Control_Systems).
- [16] A. Tuladhar, H. Jin, T. Unger and K. Mauch, "Parallel operation of single phase inverter modules with no control interconnections," in Proc. Con\$ Rec. APEC, Feb. 1997, pp. 94-100.
- [17] Hierieracal control of intellegent microgrid.
- [18] A. Tuladhar, Advanced Control Techniques for Parallel Inverter Operation Without Control Interconnections, Dept of Electrical and Computer Engineering, The University of British Columbia, 2000.
- [19] M. Prodanovic, T.C. Green, H. Mansir, A survey of control methods for threephase inverters in parallel connection, in: Eighth International Conference on Power Electronics and Variable Speed Drives, 2000.
- [20] R. Majumder, et al., Load sharing with parallel inverters in distributed generation and power system stability, in: Smart Systems 2007 "Technology, Systems and Innovation", 2007.
- [21] A. Tuladhar, Advanced Control Techniques for Parallel Inverter Operation Without Control Interconnections, Dept of Electrical and Computer Engineering, The University of British Columbia, 2000.
- [22] C.-C. Hua, K.-A.L., J.-R. Lin, Parallel operation of inverters for distributed photovoltaic power supply system, in: IEEE Annual Power Electronics Specialists Conference.
- [23] H. Tao, J. L. Duarte, and M. A. Hendrix, "Line-interactive UPS using a fuel cell as the primary source," *IEEE Transactions on Industrial Electronics*, vol. 55, pp. 3012-3021, Jul 2008.
- [24] "IEEE Standard for Interconnecting Distributed Resources with Electric Power Systems, IEEE Standard 1547, p. 16.," 2003.
- [25] Anil Tuladhar, Hua Jin, Tom Unger and Konrad Mauch, "Control of parallel inverters in distributed ac power systems with consideration of line impedance effect," *IEEE Trans. Ind. Applicat.*, vol. 36, pp. 131-138, Jan./Feb.2000.

# APPENDIX A

## GLOSSARY

<b>A</b>	<b>AC</b>	Alternating Current
	<b>ASD</b>	Adjustable Speed Drive
<b>C</b>	<b>CPU</b>	Central Processing Unit
	<b>CSI</b>	Current Source Inverter
<b>D</b>	<b>CM</b>	Common Mode
	<b>DG</b>	Distributed Generation.
	<b>DC</b>	Direct Current
	<b>DER</b>	Distributed Energy Resources
	<b>DG</b>	Distributed Generation
<b>E</b>	<b>ESS</b>	Energy Storage System.
	<b>EMC</b>	Electromagnetic Compatibility
<b>I</b>	<b>IGBT</b>	Insulated Gate Bipolar Translator
<b>P</b>	<b>PCC</b>	Point of Common Coupling.
	<b>PCM</b>	Power Control Mode
	<b>PMS</b>	Power Management System
	<b>PI</b>	Proportional- Integral
	<b>PID</b>	Proportional- Integral –Derivative
	<b>PM</b>	Permanent Magnet
	<b>PV</b>	Photo Voltaic
<b>PWM</b>	Pulse width modulation	

	<b>P</b>	Real Power
<b>Q</b>	<b>Q</b>	Reactive power
<b>R</b>	<b>RES</b>	Renewable Energy System
<b>S</b>	<b>STS</b>	Static Transfer Switch.
<b>U</b>	<b>UPS</b>	Uninterruptable Power Supply.
<b>V</b>	<b>VSI</b>	Voltage Source Inverter
	<b>VCM</b>	Voltage Control Mode
	$v$	Phase Terminal Voltages
<b>W</b>	<b>WC</b>	Wireless Control

# APPENDIX B

## SMALL SIGNAL MODEL

### B.1 State Space Equations:

The active power and the reactive power transferred from the inverter to stiff AC system is given by equations 3 and 4. In this case, these expressions includes de power losses and reactive power through inductive reactance associated with the transmission line.

$\Delta P_1 = a_1 \Delta V_1 + b_1 \Delta V_2 + c_1 \Delta \theta_1 + d_1 \Delta \theta_2$	..... (B.1)
$\Delta P_2 = a_2 \Delta V_1 + b_2 \Delta V_2 + c_2 \Delta \theta_1 + d_2 \Delta \theta_2$	.....(B.2)
$\Delta Q_1 = a_3 \Delta V_1 + b_3 \Delta V_2 + c_3 \Delta \theta_1 + d_3 \Delta \theta_2$	.....(B.3)
$\Delta Q_2 = a_4 \Delta V_1 + b_4 \Delta V_2 + c_4 \Delta \theta_1 + d_4 \Delta \theta_2$	.....(B.4)

### B.2 State space equations coefficients:

$$\begin{aligned}
 a_1 &= \frac{\partial P_1}{\partial V_1} = \frac{2 \frac{X}{R} V_{1eq} + 2V_{2eq} \sin(\theta_{1eq} - \theta_{2eq}) + \frac{X}{R} V_{2eq} \cos(\theta_{1eq} - \theta_{2eq})}{M} & a_2 &= \frac{\partial P_2}{\partial V_1} = \frac{2V_{2eq} \sin(\theta_{2eq} - \theta_{1eq}) + \frac{X}{R} V_{2eq} \cos(\theta_{2eq} - \theta_{1eq})}{M} \\
 b_1 &= \frac{\partial P_1}{\partial V_2} = \frac{2V_{1eq} \sin(\theta_{1eq} - \theta_{2eq}) + \frac{X}{R} V_{1eq} \cos(\theta_{1eq} - \theta_{2eq})}{M} & b_2 &= \frac{\partial P_2}{\partial V_2} = \frac{2 \frac{X}{R} V_{2eq} + 2V_{1eq} \sin(\theta_{2eq} - \theta_{1eq}) + \frac{X}{R} V_{1eq} \cos(\theta_{2eq} - \theta_{1eq})}{M} \\
 c_1 &= \frac{\partial P_1}{\partial \theta_1} = \frac{2V_{1eq} V_{2eq} \cos(\theta_{1eq} - \theta_{2eq}) - \frac{X}{R} V_{1eq} V_{2eq} \sin(\theta_{1eq} - \theta_{2eq})}{M} & c_2 &= \frac{\partial P_2}{\partial \theta_1} = \frac{-2V_{1eq} V_{2eq} \cos(\theta_{2eq} - \theta_{1eq}) + \frac{X}{R} V_{1eq} V_{2eq} \sin(\theta_{2eq} - \theta_{1eq})}{M} \\
 d_1 &= \frac{\partial P_1}{\partial \theta_2} = -c_1 & d_2 &= \frac{\partial P_2}{\partial \theta_2} = -c_2 \\
 a_3 &= \frac{\partial Q_1}{\partial V_1} = \frac{2(\frac{X^2}{R^2} + 2)V_{1eq} - 2V_{2eq} \cos(\theta_{1eq} - \theta_{2eq}) + \frac{X}{R} V_{2eq} \sin(\theta_{1eq} - \theta_{2eq})}{M} & a_4 &= \frac{\partial Q_2}{\partial V_1} = \frac{-2V_{2eq} \cos(\theta_{2eq} - \theta_{1eq}) + \frac{X}{R} V_{2eq} \sin(\theta_{2eq} - \theta_{1eq})}{M} \\
 b_3 &= \frac{\partial Q_1}{\partial V_2} = \frac{-2V_{1eq} \cos(\theta_{1eq} - \theta_{2eq}) + \frac{X}{R} V_{1eq} \sin(\theta_{1eq} - \theta_{2eq})}{M} & b_4 &= \frac{\partial Q_2}{\partial V_2} = \frac{2(\frac{X^2}{R^2} + 2)V_{2eq} - 2V_{1eq} \cos(\theta_{2eq} - \theta_{1eq}) + \frac{X}{R} V_{1eq} \sin(\theta_{2eq} - \theta_{1eq})}{M} \\
 c_3 &= \frac{\partial Q_1}{\partial \theta_1} = \frac{2V_{1eq} V_{2eq} \sin(\theta_{1eq} - \theta_{2eq}) + \frac{X}{R} V_{1eq} V_{2eq} \cos(\theta_{1eq} - \theta_{2eq})}{M} & c_4 &= \frac{\partial Q_2}{\partial \theta_1} = \frac{-2V_{1eq} V_{2eq} \sin(\theta_{2eq} - \theta_{1eq}) - \frac{X}{R} V_{1eq} V_{2eq} \cos(\theta_{2eq} - \theta_{1eq})}{M} \\
 d_3 &= \frac{\partial Q_1}{\partial \theta_2} = -c_3 & d_4 &= \frac{\partial Q_2}{\partial \theta_2} = -c_4
 \end{aligned}$$

where  $M = 4X + \frac{X^3}{R^2}$

### B.3 state space model:

$$[A_1] = \begin{bmatrix} 0 & 1 & 0 & 0 & 0 & 0 & 0 & 0 & 0 & 0 \\ 0 & 0 & 0 & 1 & 0 & 0 & 0 & 0 & 0 & 0 \\ \frac{k_o c_1}{\tau} & -\frac{k_o d_1}{\tau} & -\frac{1}{\tau} & 0 & -\frac{k_o a_1}{\tau} & -\frac{k_o b_1}{\tau} & 0 & 0 & 0 & 0 \\ \frac{k_o c_2}{\tau} & -\frac{k_o d_2}{\tau} & 0 & -\frac{1}{\tau} & -\frac{k_o a_2}{\tau} & -\frac{k_o b_2}{\tau} & 0 & 0 & 0 & 0 \\ -\frac{k_o c_3}{\tau} & -\frac{k_o d_3}{\tau} & 0 & 0 & -\frac{(1+k_o a_3)}{\tau} & -\frac{k_o b_3}{\tau} & 0 & 0 & 0 & 0 \\ -\frac{k_o c_4}{\tau} & -\frac{k_o d_4}{\tau} & 0 & 0 & -\frac{k_o a_4}{\tau} & -\frac{(1+k_o b_4)}{\tau} & 0 & 0 & 0 & 0 \\ \frac{c_1}{\tau} & \frac{d_1}{\tau} & 0 & 0 & \frac{a_1}{\tau} & \frac{b_1}{\tau} & -\frac{1}{\tau} & 0 & 0 & 0 \\ \frac{c_2}{\tau} & \frac{d_2}{\tau} & 0 & 0 & \frac{a_2}{\tau} & \frac{b_2}{\tau} & 0 & -\frac{1}{\tau} & 0 & 0 \\ \frac{c_3}{\tau} & \frac{d_3}{\tau} & 0 & 0 & \frac{a_3}{\tau} & \frac{b_3}{\tau} & 0 & 0 & -\frac{1}{\tau} & 0 \\ \frac{c_4}{\tau} & \frac{d_4}{\tau} & 0 & 0 & \frac{a_4}{\tau} & \frac{b_4}{\tau} & 0 & 0 & 0 & -\frac{1}{\tau} \end{bmatrix}$$



# APPENDIX C

## PARTICLE SWARM OPTIMIZATION

### C.1 Particle Swarm Optimization program:

```
clear
clc
n = 10;           % Size of the swarm " no of birds "
bird_setp = 50;  % Maximum number of "birds steps"
dim = 2;         % Dimension of the problem

c2 = 1.2;        % PSO parameter C1
c1 = 0.12;       % PSO parameter C2
w = 0.9;         % pso momentum or inertia
fitness = 0 * ones(n, bird_setp);

R1 = rand(dim, n);
R2 = rand(dim, n);
current_fitness = 0 * ones(n, 1);

current_position = 10 * (rand(dim, n) - .5);
velocity = .3 * randn(dim, n);
local_best_position = current_position;

for i = 1:n
    current_fitness(i) = tracklsq(current_position(:, i));
end

local_best_fitness = current_fitness;
[global_best_fitness, g] = min(local_best_fitness);

for i = 1:n
    global_best_position(:, i) = local_best_position(:, g);
end
```

```

velocity = w *velocity + c1*(R1.*(local_best_position-
current_position)) + c2*(R2.*(globl_best_position-
current_position));

current_position = current_position + velocity ;

iter = 0 ;
while ( iter < bird_setp )
iter = iter + 1;

for i = 1:n,
current_fitness(i) = tracklsq(current_position(:,i)) ;
end

for i = 1 : n
    if current_fitness(i) < local_best_fitness(i)
        local_best_fitness(i) = current_fitness(i);
        local_best_position(:,i) = current_position(:,i)
    ;
    end
end

[current_global_best_fitness,g] = min(local_best_fitness);

if current_global_best_fitness < global_best_fitness
    global_best_fitness = current_global_best_fitness;

    for i=1:n
        globl_best_position(:,i) = local_best_position(:,g);
    end
end

velocity = w *velocity + c1*(R1.*(local_best_position-
current_position)) + c2*(R2.*(globl_best_position-
current_position));
current_position = current_position + velocity;

sprintf('The value of interation iter %3.0f ', iter );

end

xx=fitness(:,50);

```

```
[Y,I] = min(xx);
current_position(:,I)
```

```
function F = tracklsq(pid)
    % Track the output of optsim to a signal of 1

    % Variables a1 and a2 are shared with RUNTRACKLSQ
    Kp = pid(1);
    Ki = 0;
    Kd = pid(2);

    sprintf('The value of interation Kp= %3.0f, Kd=
%3.0f', pid(1),pid(2));
    % Compute function value
    simopt =
simset('solver','ode5','SrcWorkspace','Current','DstWorkspace'
,'Current'); % Initialize sim options
    [tout,xout,yout] = sim('inverter_pwm22',[0
100],simopt);
    e=yout-1 ; % compute the error
    sys_overshoot=max(yout)-1; % compute the overshoot

    alpha=10;beta=10;
    F=e2*beta+sys_overshoot*alpha;

end
```